CHAPTER 3

SIMULATION AND VALIDATION

A dust dispersion model is usually based on Gaussian distribution. There are various models available like AERMOD, CALPUFF, ADAMS, FDM etc. to predict dust dispersal from a mining activity. It was found that AERMOD is a most suitable tool for mining industry based on review of literature. AERMOD is a steady-state plume model to predict dust concentration due to various sources. In the stable boundary layer (SBL), it assumes the concentration distribution to be Gaussian in both the vertical and horizontal directions. In the convective boundary layer (CBL), the horizontal distribution is assumed to be Gaussian, but the vertical distribution is described with a bi-Gaussian probability density function (Willis and Deardorff, 1981 and Briggs, 1993). This assumption was also incorporated in AERMOD.

One of the major improvements that AERMOD brings to applied dispersion modelling is its ability to characterize the planetary boundary layer (PBL) through both surface and mixed layer scaling. AERMOD constructs vertical profiles of required meteorological variables based on measurements and extrapolations of those measurements using similarity (scaling) relationships. Vertical profiles of wind speed, wind direction, turbulence, temperature, and temperature gradient are estimated using all available meteorological observations (Cimorelli et. al., 2004).

3.1 AERMOD modelling system

AERMOD modelling system consists of one main program (AERMOD) and two pre-processors (AERMET and AERMAP). The major purpose of AERMET is to calculate boundary layer parameters to be used by AERMOD. The meteorological interface, internal to AERMOD, uses these parameters to generate profiles of the needed meteorological variables. In addition, AERMET passes all meteorological observations to AERMOD. Surface characteristics in the form of albedo, surface roughness and bowen ratio and standard meteorological observations (wind speed, wind direction, temperature, and cloud cover) are input to AERMET. AERMET then calculates the PBL parameters i.e. friction velocity, Monin-Obukhov length,

convective velocity scale, temperature scale, mixing height and surface heat flux. These parameters are then passed to the interface (which is within AERMOD) where similar expressions (in conjunction with measurements) are used to calculate vertical profiles of wind speed, lateral and vertical turbulent fluctuations, potential temperature gradient and potential temperature. The terrain pre-processor, AERMAP uses gridded terrain data to calculate a representative terrain-influence height, also referred to as the terrain height scale. The terrain height scale, which is uniquely defined for each receptor location, is used to calculate the dividing streamline height. The gridded data needed by AERMAP is selected from Digital Elevation Model (DEM). AERMAP is also used to create receptor grids. The elevation for each specified receptor is automatically assigned through AERMAP. Subsequently, AERMAP passes this information to AERMOD (Cimorelli et. al., 2004).

3.2 Simulation procedure for a mine to predict dust dispersal

The dust dispersal simulation of a surface mine from different mining activities, requires a certain procedure to be followed. The base map of the mine along with the nearby surrounding area, which can be polluted from the mining activities, is a prime requirement of the simulation. This can be provided in local coordinate system or global coordinate system.

Every mining activity, particularly related to surface mining, directly or indirectly contribute to the problem of air pollution. Secondly, information about the potential dust sources is to be provided. This information includes sources strength, source dimension, type of source and source dimension.

In the next step of simulation, one has to provide location of the receptor, where concentration of the air pollutant is to be predicted or calculated. It may be provided in the form of grid or discrete point depending on the requirement. This is required to predict the concentration of an air pollutant at a particular location or contours of concentration in the area provided as base map to be influenced by mining activities.

Surface meteorological data, which are collected from the field or observed from a station cannot be directly used in AERMOD. These are required to be pre-processed in any model. AERMET is a pre-processor which come with the AERMOD and generates the file which can be used in the AERMOD as input for the

meteorological data. AERMET processor was used to develop two types of input files for AERMOD.

Surface file (*.SFC): It contains hourly estimates of boundary layer parameters which are derived from the surface meteorological parameters.

Profile file (*.PFL): It contains multiple level observations of wind speed, wind direction, temperature and standard deviation of the fluctuating wind components.

Meteorological parameters are another set of data required for simulation of dust dispersal from an area or mine. There are two type of meteorological data required for simulation: Surface meteorological data and Upper air meteorological data. Opaque cloud cover, dry bulb temperature, wind direction and wind speed are the four important surface meteorological data required for simulation also termed as Primary surface meteorological data. The surface meteorological data, other than primary surface meteorological data are also required for simulation. However, secondary meteorological data can be estimated with the help of primary surface meteorological data. It is always advisable to use measured secondary surface meteorological data for better accuracy.

All parameters of upper air meteorological data is required for simulation. These should be collected from a nearby weather station.

Digital elevation model (DEM) of the area is also required for simulation. DEM is a model or set of data contains the terrain contours of the area considered for simulation. This can be provided initially along with the base map or separately by a pre-processor provided in the model. Simulation process predicts dust dispersal with good accuracy, if the elevation of all the discrete points falling in the base map area will be provided as a digital elevation model.

Based on the above parameters, one can predict dust concentration from a simulated mining system.

3.3 Simulation of an opencast coal mine 'A' to predict dust dispersal

A surface coal mine Mine 'A' was chosen for this study. This mine is located in the Ib valley Coalfield situated near Jharsuguda, Odisha, India. The coalfield has large reserves of coal suitable for power generation and extends over an area of about 1400 km^2. Its strike line swings from north-south to east–west in the southern and northern extremes. The geology of the area mainly comprises of Lower Gondwana system.

3.3.1 Description of Mine 'A' Opencast Coal Project

Figure 3.1 shows the satellite image of the Mine 'A'. Some villages are also near the mine.

The total geological reserve is 422 MT, mineable reserve 358.58 MT and extractable reserve is 269.35 Mt. The extraction is around 90%. The coal grades ranges from Grade F to G. In the area chosen for open cast mining under Mine 'A', only one seam is proposed to be worked. The thickness of the coal seam, varies from 25-35 m and maximum thickness of the seam is 33.53 m. There are several dirt bands, existing in mining project. The dirt bands are of combustible carbonaceous shale of thickness vary from 1.47 m to 6.91 m. One such thick band persists in the lower half of the seam throughout the block. Thickness of bands tend to increase towards south as well as towards west of the mine. The average working stripping ratio is 2.34 and average Gradient is 1 in 18 to 1 in 10.

Selective mining approach is being adopted due to presence of a number of dirt bands in the project. Surface Miner have been used for mining of coal (Make: Wirtgen, model: 2100 SM & 2200 SM). Their maximum cutting depth are 250 mm and 350 mm and rated capacities are 550 and 668 m^3/hr respectively. Tippers are being used for transporting material from pit to surface and surface to siding and pay loaders are being used for transporting material from siding to loading point.

Figure 3.1: Satellite image of Mine 'A' Opencast Coal Project

3.3.2 Dust Sources and their location

The important dust sources inside the mine as well as outside the mine have been identified. The first step in simulation of any coal mine for dispersion of dust is identification of significant dust sources and classify them in terms of line, point, line area, area sources etc. These are 22 in numbers. Out of these 22 sources, four are coal faces, two external dumps and seven internal dumps, two coal stock yards, five haul roads and two belt conveyors in a coal handling plant. Among four coal faces, two are at north-east extension and two are at the south-west production of the mine. Two external dumps are at the south side of the mine and internal dumps are almost in the centre of the mine. Coal stock yards and coal handling plants are also at the south side of the mine. Four coal faces were considered as point sources. Two external dumps namely OBE1 & OBE2 with an area of 17.50 ha and a maximum height of 50 m and average height of 45 m were considered as area polygon sources. Seven internal dumps namely OB I, OB II, OB III, OB IV, OB V, OB VI & OB VII with quantity of 140.1432 Mm^3 in an area of 275.700 ha with height of 50 m (OB I, OB V & OB VII) and 85 m (OB II, OB III, OB IV & OB VI) were also considered as area polygon sources. Two coal stock yards were considered as area polygon sources and five haul roads were considered as line area sources. Belt of coal handling plants (B1 & B2) were considered as line sources. Table 3.1 summarises the dust sources with type and dimension considered for simulation.

Table 3.1: Dust sources with their type and dimension

S. No.	Source Id	Type of Source	Dimension/ Height (m)
1.	COALFACE1	Point	1
2.	COALFACE2	Point	1
3.	COALFACE3	Point	1
4.	COALFACE4	Point	1
5.	OBE1	Area Polygon	50
6.	OBE2	Area Polygon	50
7.	OBI	Area Polygon	50
8.	OBII	Area Polygon	85
9.	OBIII	Area Polygon	85
10.	OBIV	Area Polygon	85
11.	OBV	Area Polygon	50
12.	OBVI	Area Polygon	85
13.	OBVII	Area Polygon	50

14.	COALSTOCK1	Area Polygon	30
15.	COALSTOCK2	Area Polygon	30
16.	HAUL1	Line Area	3400
17.	HAUL2	Line Area	2900
18.	HAUL3	Line Area	1900
19.	HAUL4	Line Area	410
20.	HAUL5	Line Area	2200
21.	B1	Line	3
22.	B2	Line	1.5

3.3.3 Determination of source strength of dust sources

Dust sources identified for simulation were superimposed on the base map of the study. However, only few can be considered as significant sources of dust. Emission rates or factors is the primary concern for an assessment of the hazard due to these activities. The source strength are nothing but the emission factor of different mining activities. Emission factor is the emission rate of a source at which it is emitting a particular air pollutant. Various authors had carried out research to correlate mining activities with emission factor. Chakraborty et al., (2002) had given the empirical relationship to calculate the emission factor of various mining activities of Indian coal mines. These equations have been used for present work and they are summarised in Table 3.2 given below. In the next step, source strength of each source was estimated from the emission factor equations given by Chakraborty et al. (2002), shown in Table 3.3. The parameters required to calculate the emission factor from these equations are summarised in Appendix I.

These are high for the haul road and coal faces then for overburden and coal stocks. Emission rate of haul road is highest due to continuous erosion of haul road from the movement of vehicle on it. Whereas these emission rates are high for coal face due to continuous cutting of the coal and discharge on the dumpers. In case of overburden erosion usually takes place due to wind although it is continuous but it emits less dust due to low wind velocity in the area.

Table 3.2: Emission Factors of Different Mining Activities (Chakraborty et al., 2002)

Activity	**Empirical Equation**
Coal/mineral loading	$E=[\{(100-m)/m\}^{0.1}\{s/(100-s)\}^{0.3}h^{0.2}\{u/(0.2+1.05u)\}\{xl/(15.4+0.87xl)\}]$
Coal/mineral unloading	$E=0.023[\{(100-m)sh\}/\{m(100-s)\}]^2(u^3cy)^{0.1}$
Haul road	$E=[\{(100-m)/m\}^{0.8}\{s/(100-s)\}^{0.1}u^{0.3}\{2663+0.1(v+fc)\}10^{-6}]$
Exposed overburden dump	$E=[\{(100-m)/m\}^{0.2}\{s/(100-s)\}^{0.1}\{u/(2.6+120u)\}\{a/(0.2+276.5a)\}]$
Stock yard	$E=\{(100-m)/m\}^{0.1}\{s/(100\ s)\}\{u/(71+43u)\}[\{cy/(329+7.6cy)\}+\{lx/(30+900\ lx)\}]$
Coal handling plant	$E=[\{(100-m)/m\}^{0.4}\{a^2s/(100-s)\}^{0.3}\{u/(160+3.7u)\}]$

where

m = Moisture content (%)
s = Silt content (%)
u = Wind speed (m/s)
h = Drop height (m)
f = Frequency (no. of holes/day)
l = Size of loader (m^3)
v = Average vehicle speed (m/sec)
c = Capacity of dumper (ton)

a = Area (km^2)
y = Frequency of unloading (no. / Hr)
x = Frequency of loading (no. / Hr)
E = Emission rate (g/sec)

Table 3.3: Source strength of dust sources

S. No.	Name of the location	Emission rate
1.	COALFACE1	0.143 g/s
2.	COALFACE2	0.143 g/s
3.	COALFACE3	0.143 g/s
4.	COALFACE4	0.143 g/s
5.	OB1	2.1×10^{-6} g/s-m^2
6.	OB2	2.1×10^{-6} g/s-m^2
7.	OBI	4.3×10^{-6} g/s-m^2
8.	OBII	4.3×10^{-6} g/s-m^2
9.	OBIII	4.3×10^{-6} g/s-m^2
10.	OBIV	4.3×10^{-6} g/s-m^2
11.	OBV	4.3×10^{-6} g/s-m^2
12.	OBVI	4.3×10^{-6} g/s-m^2
13.	OBVII	4.3×10^{-6} g/s-m^2
14.	COALSTOCK1	8×10^{-6} g/s-m^2
15.	COALSTOCK2	8×10^{-6} g/s-m^2
16.	HAUL1	2.13×10^{-3} g/s-m^2
17.	HAUL2	2.13×10^{-3} g/s-m^2
18.	HAUL3	2.13×10^{-3} g/s-m^2
19.	HAUL4	2.13×10^{-3} g/s-m^2
20.	HAUL5	2.13×10^{-3} g/s-m^2
21.	B1	2.16×10^{-4} g/s-m^2
22.	B2	2.16×10^{-4} g/s-m^2

3.3.4 Location of receptors

There are four points namely, A1, A2, A3 and A4 identified as receptors, where measurement of the PM_{10} is carried out. All these points are considered as discrete receptors to estimate the concentration of PM_{10}. The receptors are shown in figure 3.2 and the co-ordinates of the location of these receptors are summarised in Table 3.6.

Figure 3.2: Receptors location in the study area of Mine 'A'

3.3.5 Meteorological parameters for Mine 'A' area

The climate of the area is dry tropical. There are four seasons, namely summer (March–May), rainy (June– August), autumn (September–November) and winter (December–February). A Meteorological Station of the Indian Meteorological Department (IMD) is located at Jharsuguda District. During the summer months the temperature reaches 47°C and in winter months it falls up to 10°C. Annual mean maximum and minimum temperatures are 33.2°C and 20.5°C, respectively. Wind velocity in the area varies from 2.28 to 4.45 m/s with an average of 3.28 m/s. The annual calm period (wind velocity < 0.6 m/s) for the area is 50% of the total duration of the day till 8:30 hrs. This calm period has reduced further to 40% of total duration of the day till 17:30 hrs. The predominant wind direction for the area is westerly. The south–west monsoon is the principal source of rainfall in the area. The average rainfall recorded at the Jharsuguda IMD station is 1400 mm/year. There are on average 81 rainy days in a year.

3.3.5.1 Surface meteorological parameters

There are several meteorological parameters which are required as input in AERMOD to provide environmental conditions for the prediction of concentration of PM_{10}. The concentration of PM_{10} was predicted for the peak winter and peak summer season. Generally in these seasons, the concentration levels of PM_{10} are highest and lowest respectively. January and May were identified as peak winter and peak summer season in year 2013. The surface meteorological data has been collected for the Jharsuguda District from Indian Meteorological Department, Pune for the above mentioned two months. The meteorological parameters used for simulation are summarise in Table 3.4.

Table 3.4: List of Surface Meteorological Parameters considered for simulation with their unit

Meteorological Parameters	Unit
Opaque Cloud Cover	Tenths
Dry Bulb Temperature	Degree Celsius(°C)
Relative Humidity	Percentage (%)
Station Pressure	Millibars (mb)
Wind Direction	Degree (°)
Wind Speed	Metre per second(m/s)

Ceiling Height	Metre(m)
Hourly Precipitation Amount	Hundredths of inches
Global Horizontal Radiation	Watt-hour per square metre (Wh/m^2)

These parameters have been collocated on hourly basis for January 2013 and May 2013 respectively. The data were divided in two sets for both the months. Each set of data consisted of 744 hours data and there are 1488 hours data collected altogether. These data are given in Appendix II.

3.3.5.2 Upper air meteorological parameters

Upper air data is necessarily required to calculate the mixing height of the air pollutant. Mixing height is the altitude above the surface where air pollutant will mix with the upper atmosphere with in troposphere. It is calculated using surface and upper air meteorological parameters. These air pollutants disperse very widely in a given region after getting mixed with upper atmosphere. The surface meteorological data were further processed along with the upper air mixing data. Upper air mixing data of the Jharsuguda district were taken from Radiosonde Dataset of Earth System Research Laboratory (ESRL), National Oceanic and Atmospheric Administration (NOAA) for the month of January and May 2013.

Wind rose diagram generated from AERMET for the month of January and May 2013 have been shown in the Figure 3.4 and 3.5 respectively. These diagrams clearly shows that predominant wind direction is westerly. The total calm period for wind velocity was 43.55 % for the month of January 2013 where it was 32.88 % for the month of May 2013.

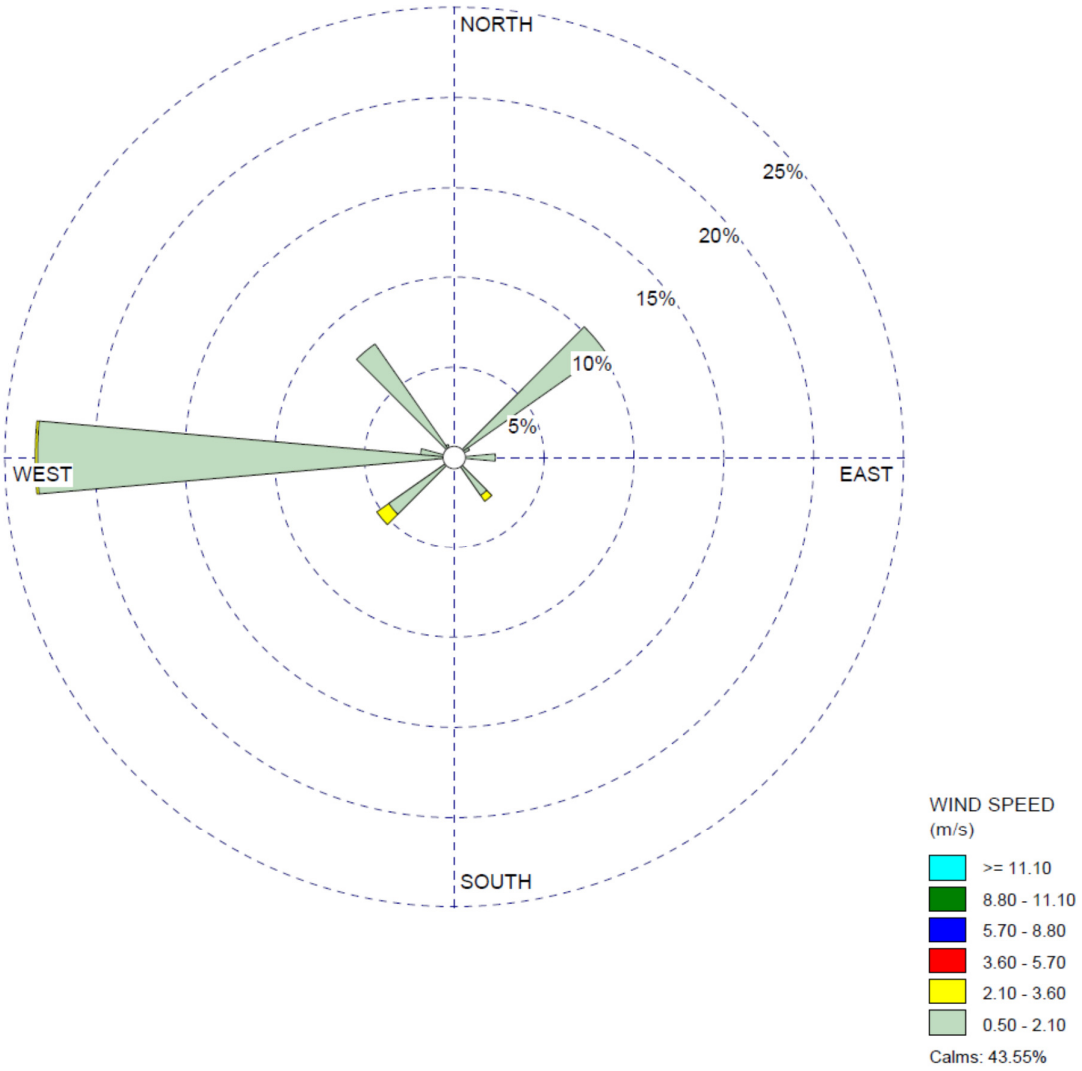

Figure 3.3: Wind - rose diagram of Jharsuguda District for the month of January 2013

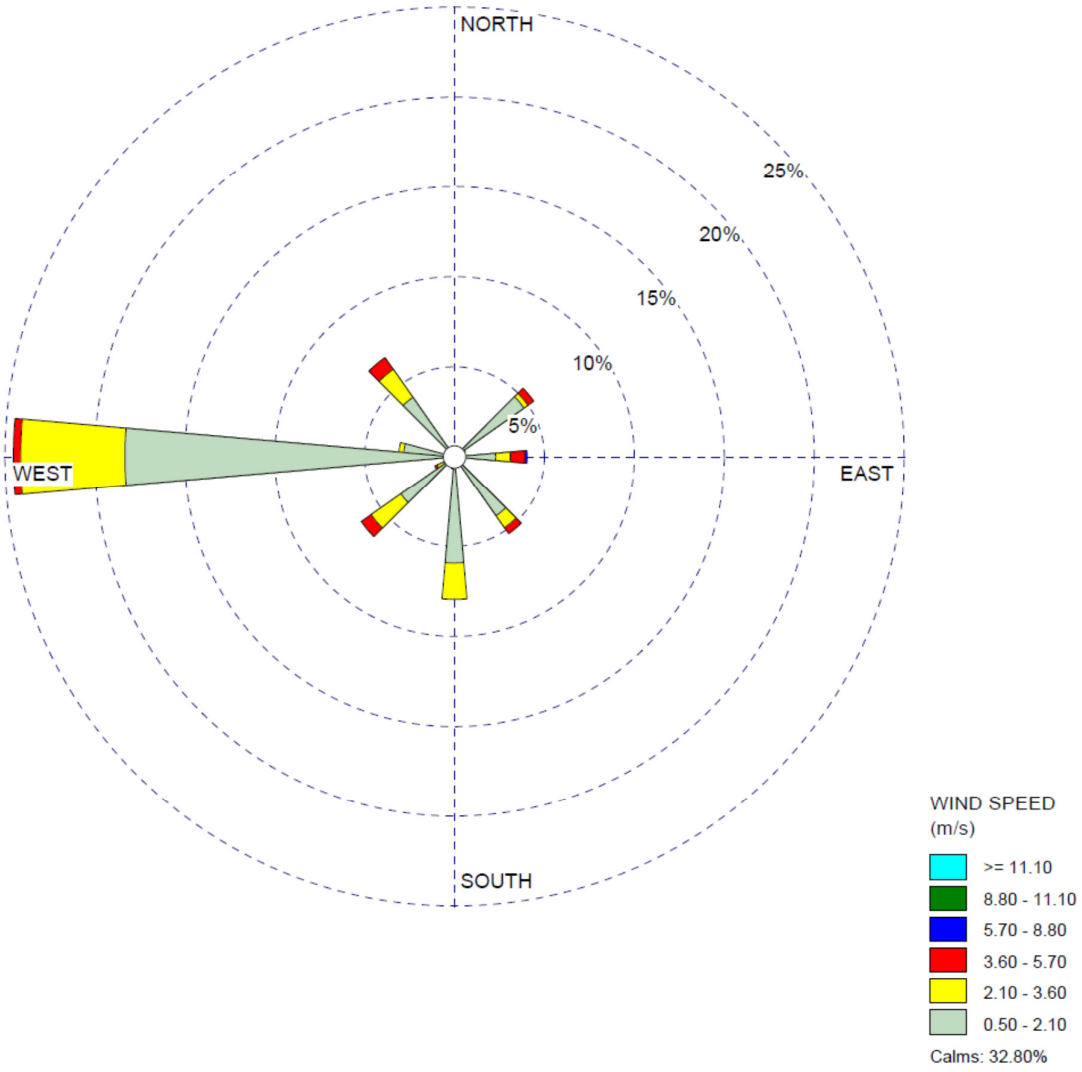

Figure 3.4: Wind - rose diagram of Jharsuguda District for the month of May 2013

3.3.6 Development of Digital Elevation Model (DEM)

Digital elevation data or terrain data is another input required in for simulation. An imagery of the mining area has been taken from United States Geological Survey (USGS) for the preparation of DEM. The resolution is limited to 30 m for this imagery. The latitude and longitude have been determined considering the area covered in the study.

The terrain data were uploaded in the model over the base map. AERMAP, which is a pre-processor in the model, was run to develop the digital elevation model of the selected area of the study. Elevation of dust sources and receptors have been calculated based on digital elevation model. The developed digital elevation model has been shown in the Figure 3.5.

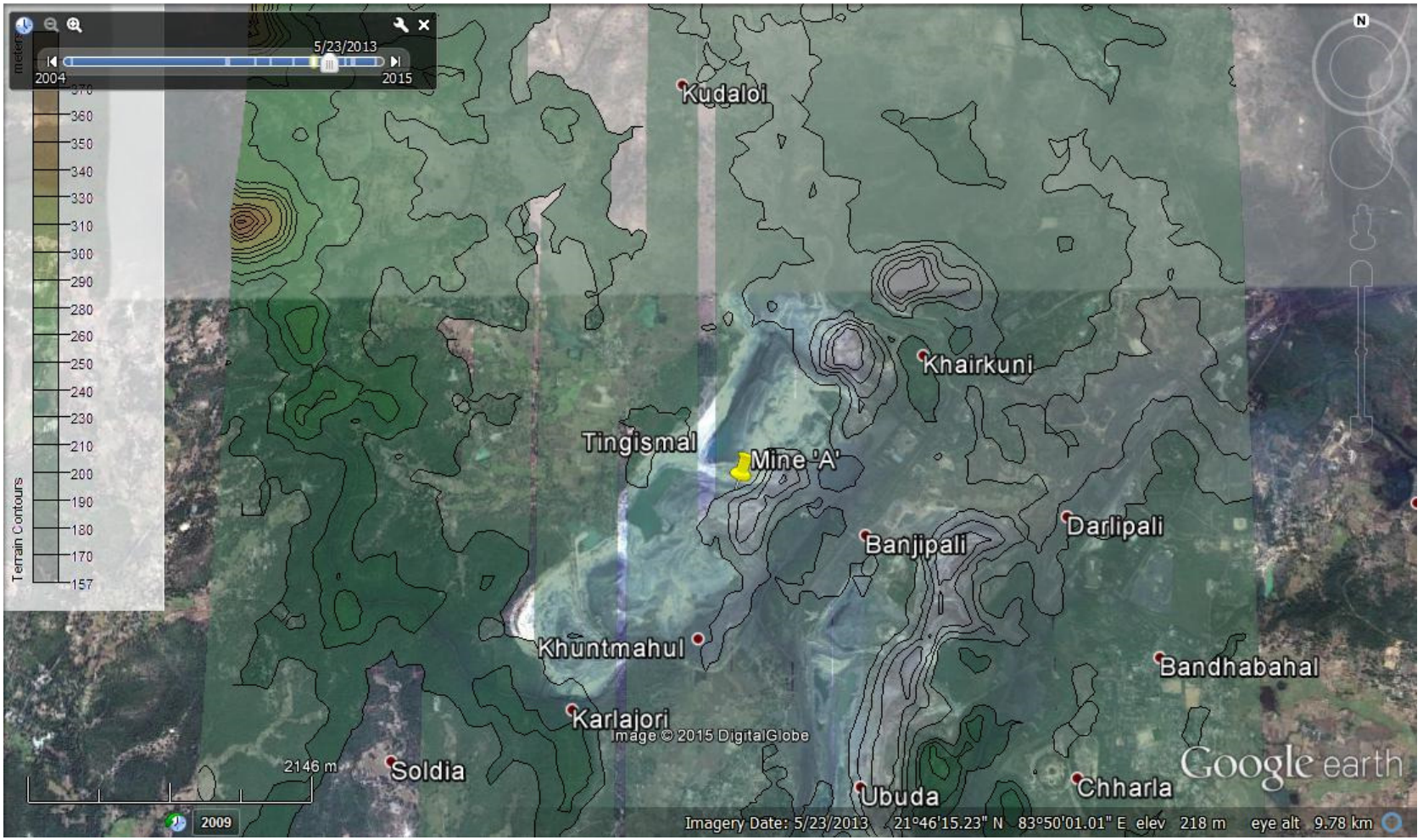

Figure 3.5: Digital Elevation Model of Mine 'A' generated by AERMAP

3.4 Prediction of concentration of PM_{10} using AERMOD at receptors

Ministry of Environment and Forest (MoEF) has enforced new National Ambient Air Quality Standards (NAAQS) in 2009. According to it, dust concentrations in the residential area and industrial area are to be measured in particulate matter of two types. These are categorised as Particulate Matter of equal or less than 10 µm (PM_{10}) and Particulate Matter of equal or less than 2.5 µm ($PM_{2.5}$). Measurement of concentration was done for PM_{10} for different time and season. These measurements were made at different receptors. The validation study can only be done with same attribute. So the predictions of the dust generation from the different dust generating sources was carried out for PM_{10} only. The concentration levels of PM_{10} were predicted for the receptors A1, A2, A3 and A4. These predictions were made for the averaging period of 24 hr (Daily basis) and monthly basis. All the predictions were done for January and May of 2013.

The concentration levels of PM_{10} have been predicted at all four receptors on daily basis and monthly basis for the month of January and May 2013. These predictions were made averaging 24 predictions on hourly basis for daily average period. Since the month of January and May contains 31 days, there are 31 highest concentrations predicted for the above mentioned months for daily averaging time period. Similarly, predictions were also made for these receptors on monthly basis by averaging daily predictions.

The predicted contour of PM_{10} concentration with inbuilt values for the month of January 2013 has been shown through figures 3.6 to 3.32.

Table No. 3.5 summarises the peak concentrations predicted for the month of January 2013 on daily basis as depicted through figures 3.6 to 3.32 mentioned above.

Similarly, the daily predicted contour of PM_{10} concentration with inbuilt values for the month of May 2013 has been shown through figures 3.33 to 3.63.

Table No. 3.6 summarises the peak concentrations predicted for the month of May 2013 on daily basis as depicted through figures 3.6 to 3.32 mentioned above.

The monthly predicted contour of PM_{10} concentration with inbuilt values for the month of January and May of 2013 has been shown in figure 3.64 and 3.65 respectively.

Table No. 3.7 summarises the concentrations predicted for the month of January and May of 2013 on monthly basis as depicted from figure 3.64 and 3.65 mentioned above.

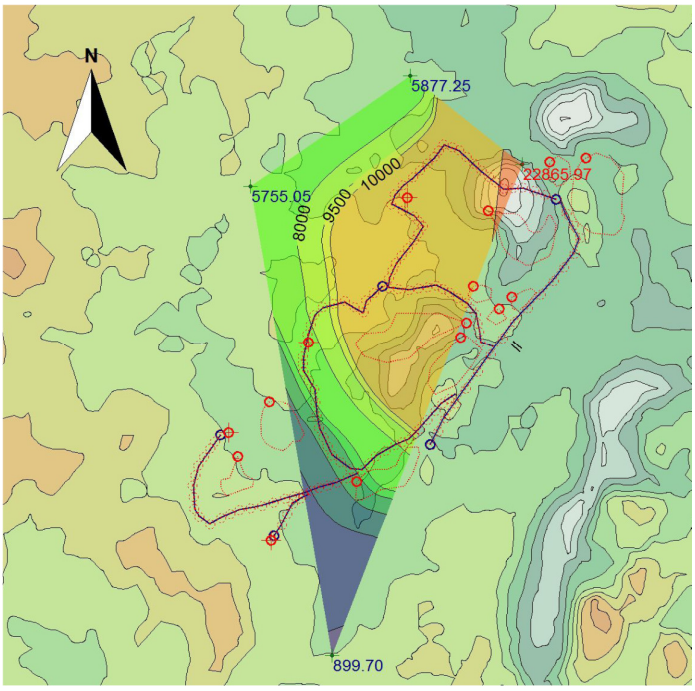

Figure 3.6: 1st Highest predicted concentration level of PM_{10} with inbuilt values for daily averaging time period in January 2013

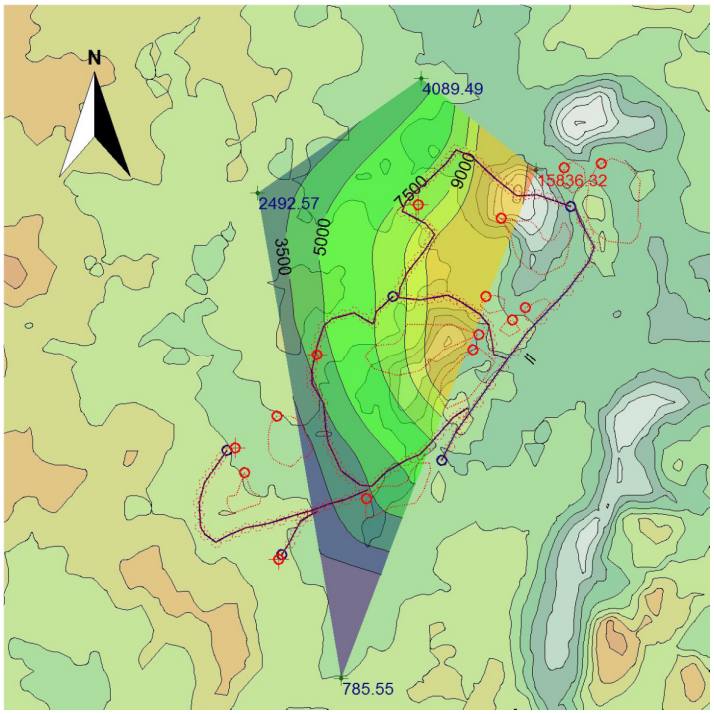

Figure 3.7: 2nd Highest predicted concentration level of PM_{10} with inbuilt values for daily averaging time period in January 2013

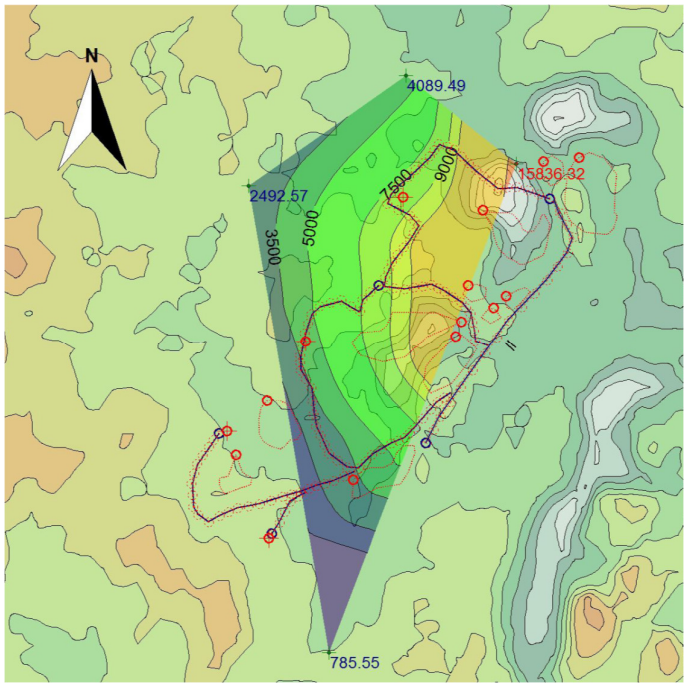

Figure 3.8: 3rd Highest predicted concentration level of PM_{10} with inbuilt values for daily averaging time period in January 2013

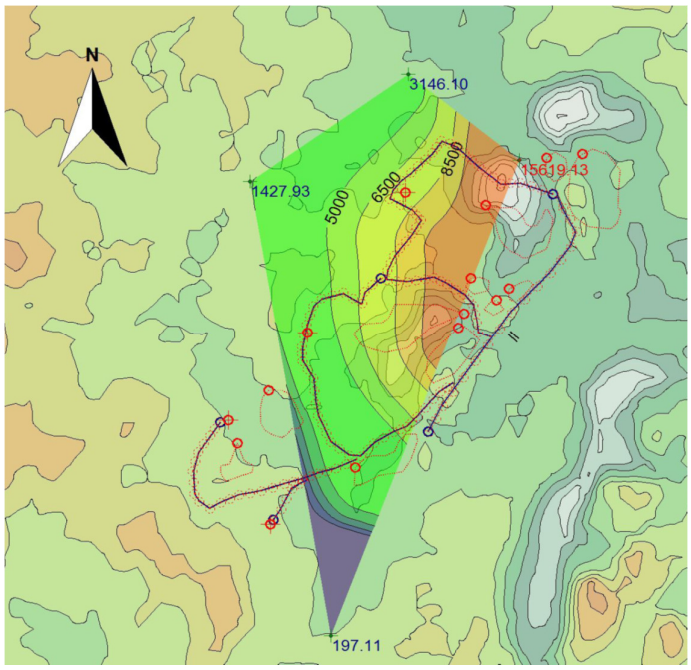

Figure 3.9: 4th Highest predicted concentration level of PM_{10} with inbuilt values for daily averaging time period in January 2013

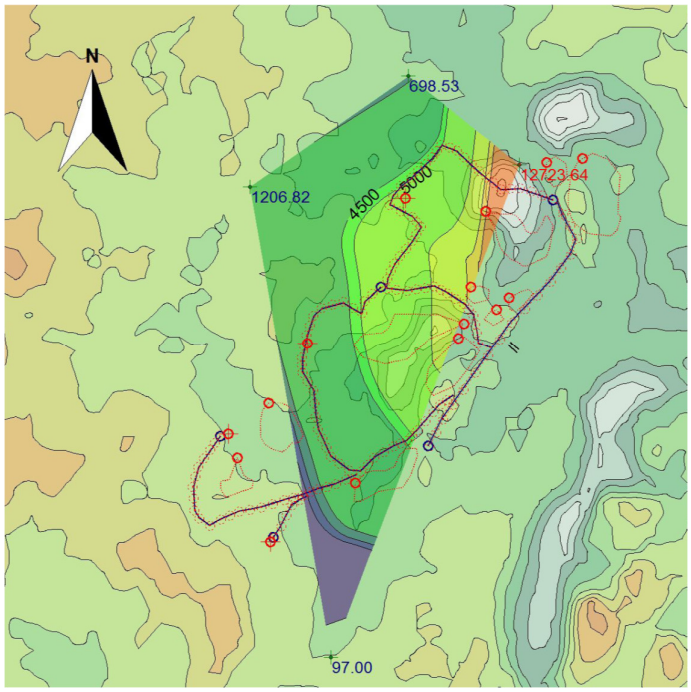

Figure 3.10: 5th Highest predicted concentration level of PM_{10} with inbuilt values for daily averaging time period in January 2013

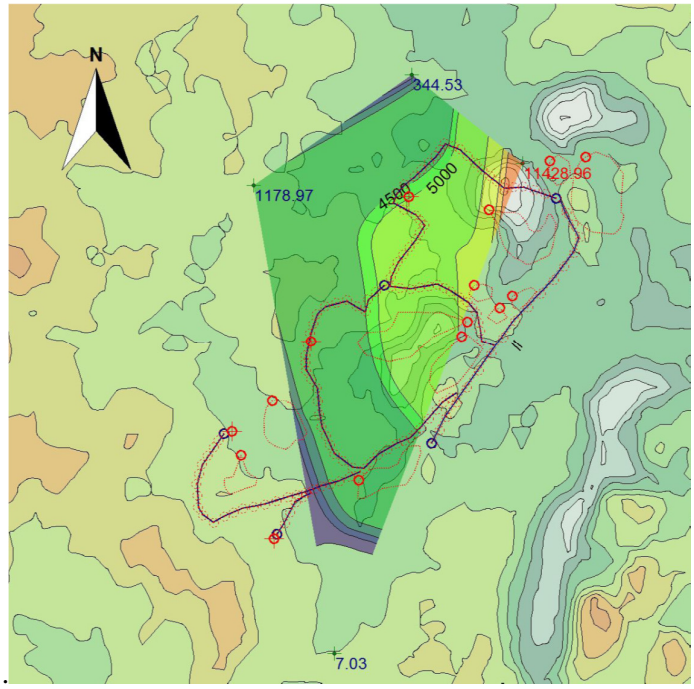

Figure 3.11: 6th Highest predicted concentration level of PM_{10} with inbuilt values for daily averaging time period in January 2013

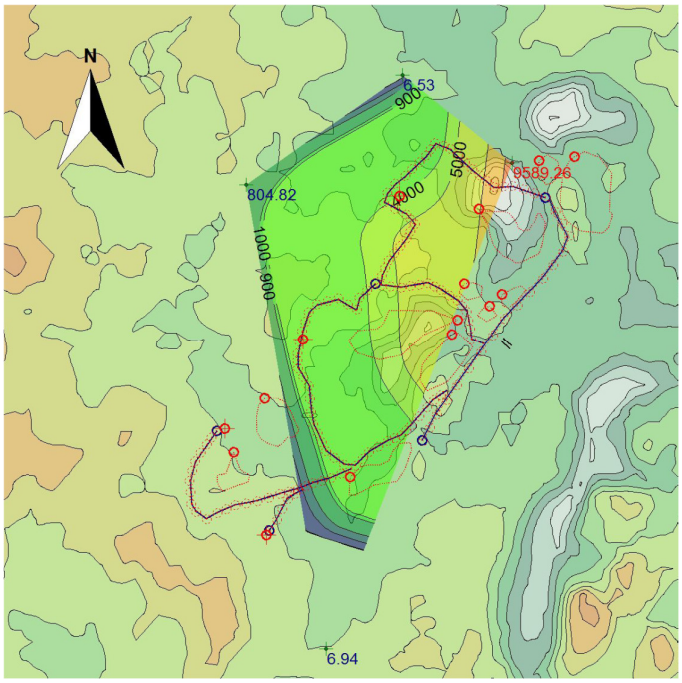

Figure 3.12: 7th Highest predicted concentration level of PM_{10} with inbuilt values for daily averaging time period in January 2013

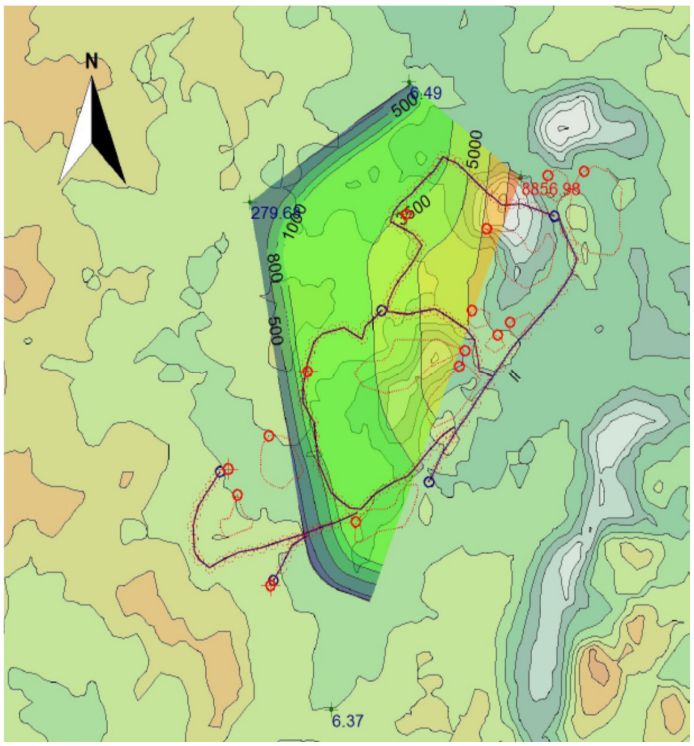

Figure 3.13: 8th Highest predicted concentration level of PM_{10} with inbuilt values for daily averaging time period in January 2013

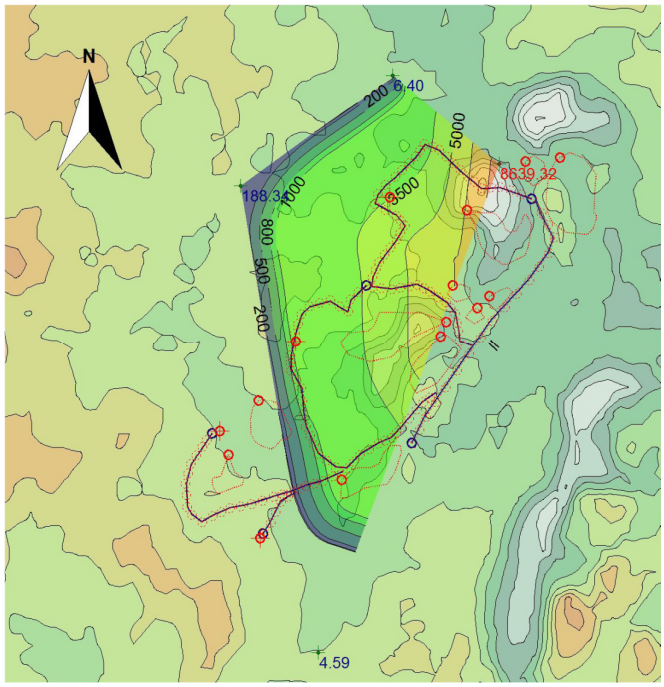

Figure 3.14: 9th Highest predicted concentration level of PM_{10} with inbuilt values for daily averaging time period in January 2013

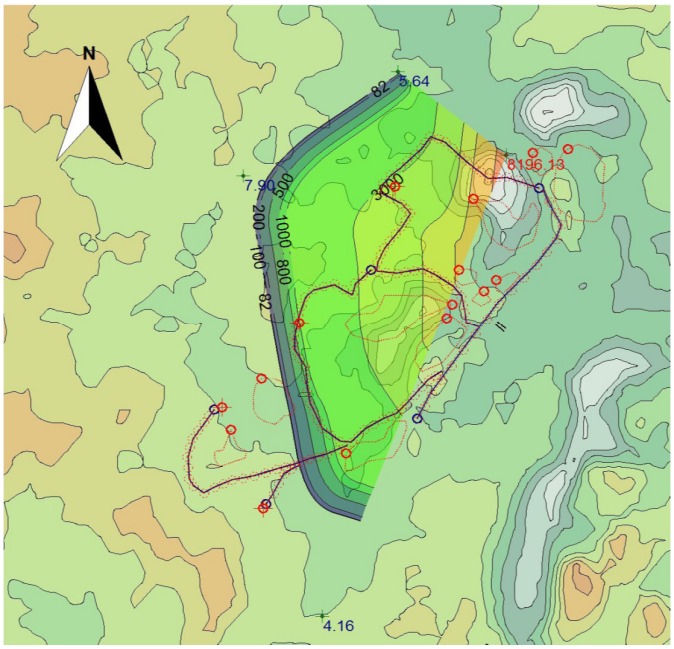

Figure 3.15: 10th Highest predicted concentration level of PM_{10} with inbuilt values for daily averaging time period in January 2013

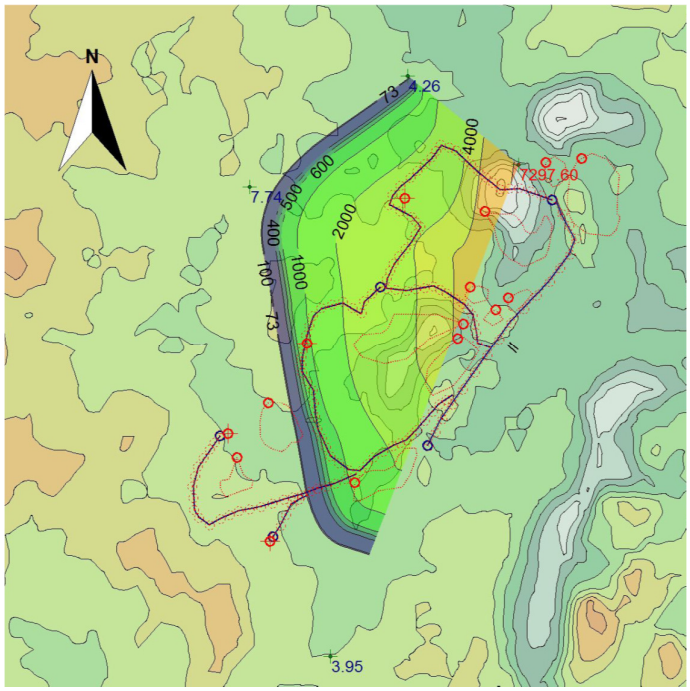

Figure 3.16: 11th Highest predicted concentration level of PM_{10} with inbuilt values for daily averaging time period in January 2013

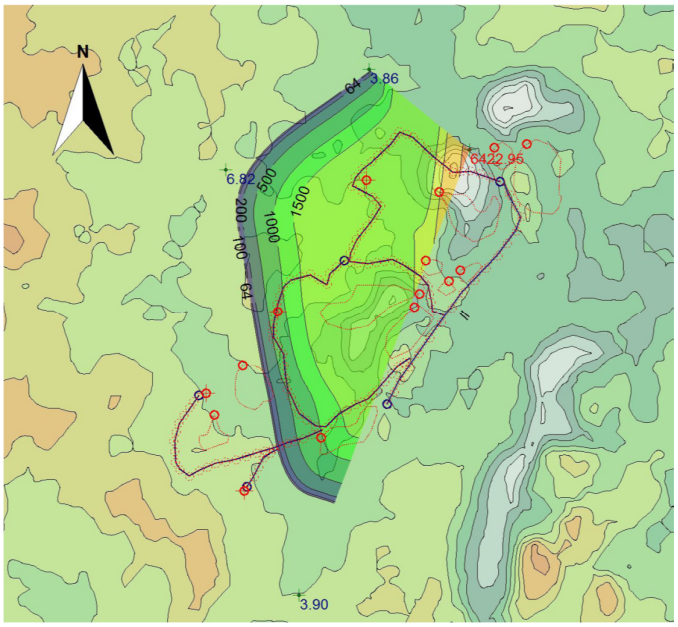

Figure 3.17: 12th Highest predicted concentration level of PM_{10} with inbuilt values for daily averaging time period in January 2013

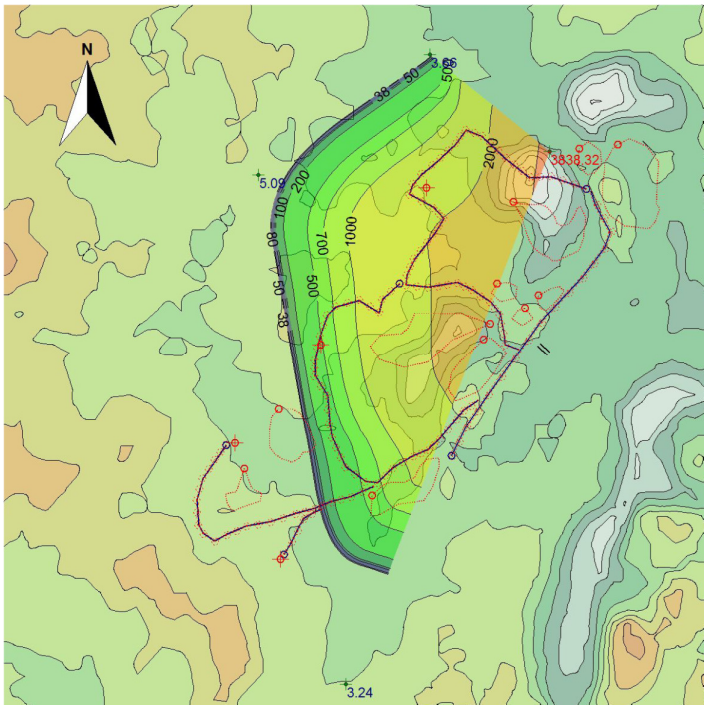

Figure 3.18: 13th Highest predicted concentration level of PM_{10} with inbuilt values for daily averaging time period in January 2013

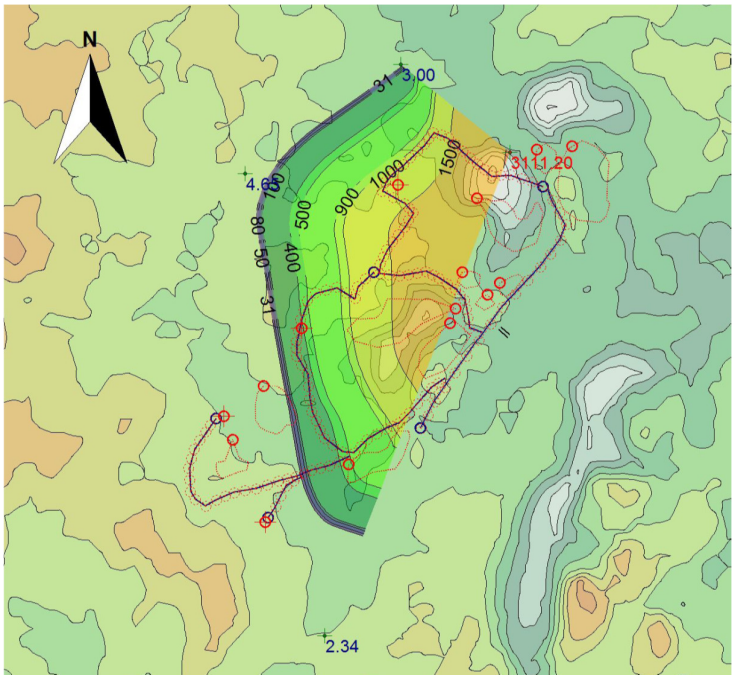

Figure 3.19: 14th Highest predicted concentration level of PM_{10} with inbuilt values for daily averaging time period in January 2013

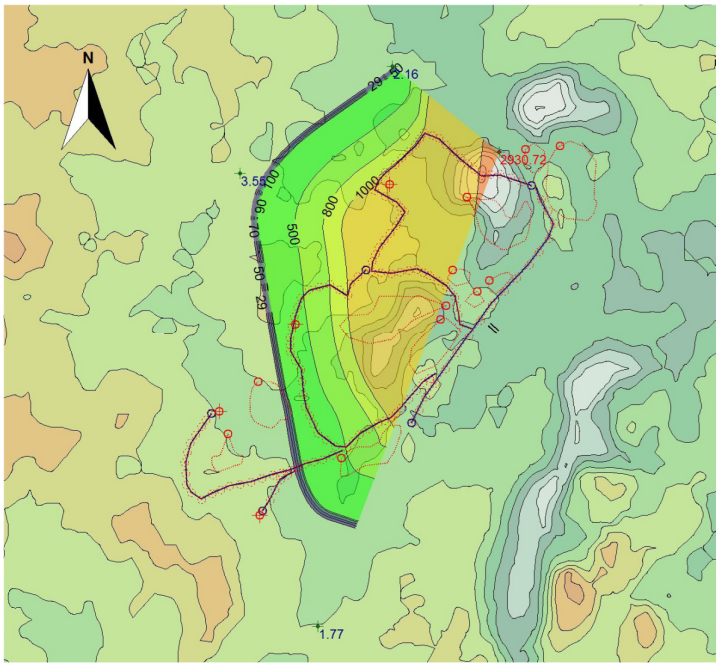

Figure 3.20: 15th Highest predicted concentration level of PM_{10} with inbuilt values for daily averaging time period in January 2013

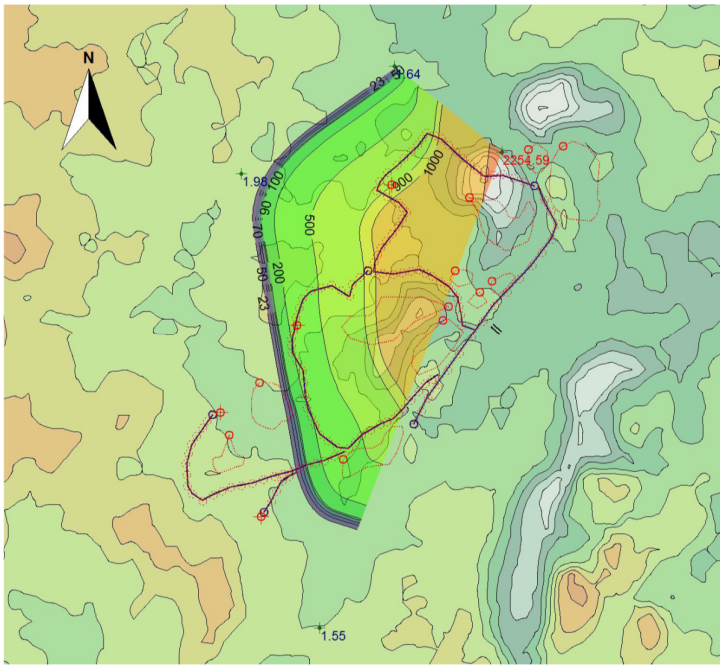

Figure 3.21: 16th Highest predicted concentration level of PM_{10} with inbuilt values for daily averaging time period in January 2013

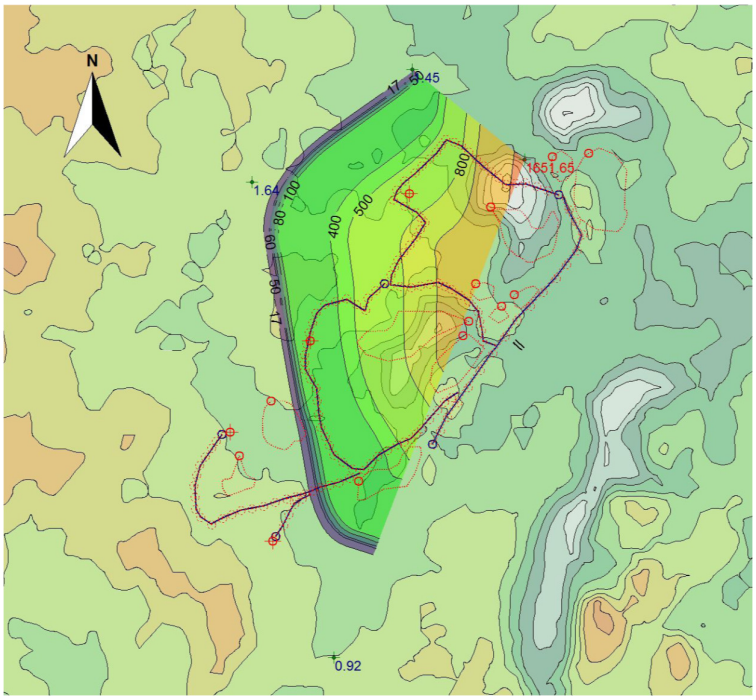

Figure 3.22: 17th Highest predicted concentration level of PM_{10} with inbuilt values for daily averaging time period in January 2013

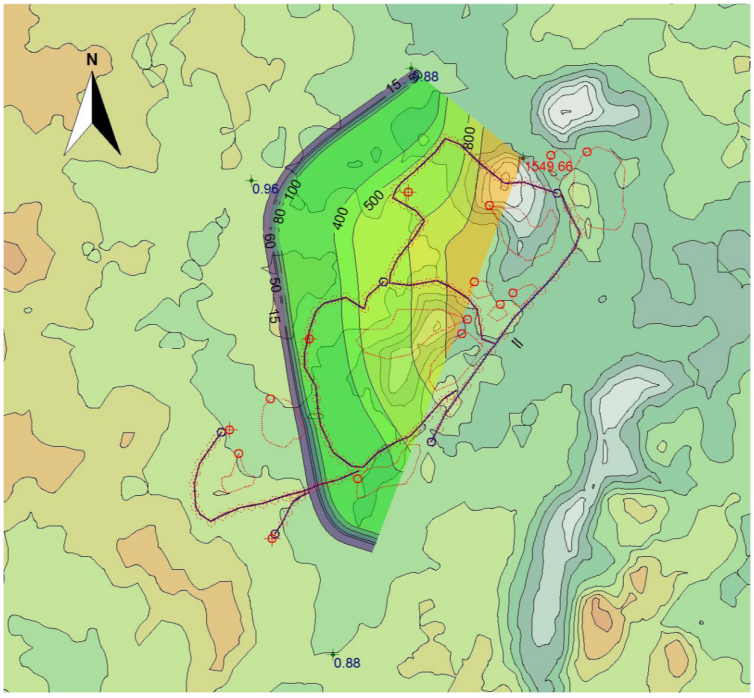

Figure 3.23: 18th Highest predicted concentration level of PM_{10} with inbuilt values for daily averaging time period in January 2013

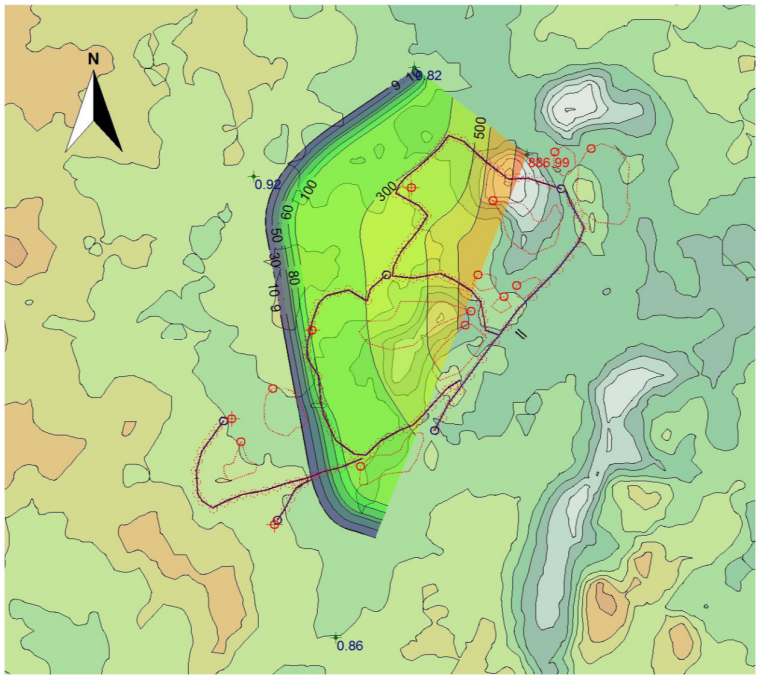

Figure 3.24: 19th Highest predicted concentration level of PM_{10} with inbuilt values for daily averaging time period in January 2013

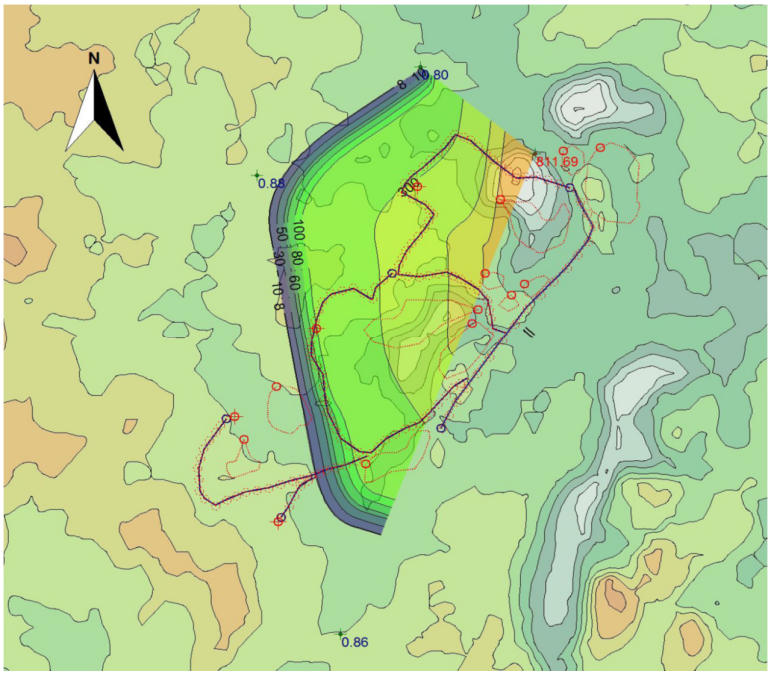

Figure 3.25:20th Highest predicted concentration level of PM_{10} with inbuilt values for daily averaging time period in January 2013

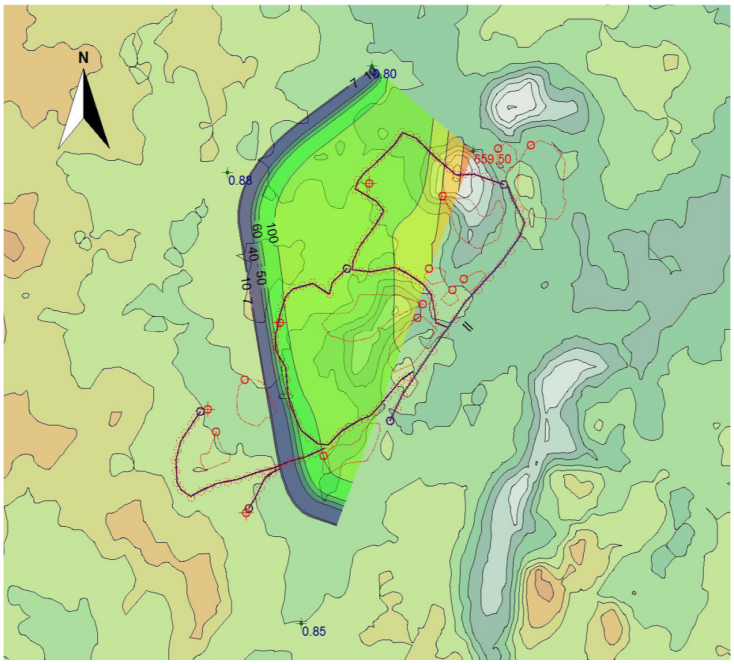

Figure 3.26:21st Highest predicted concentration level of PM_{10} with inbuilt values for daily averaging time period in January 2013

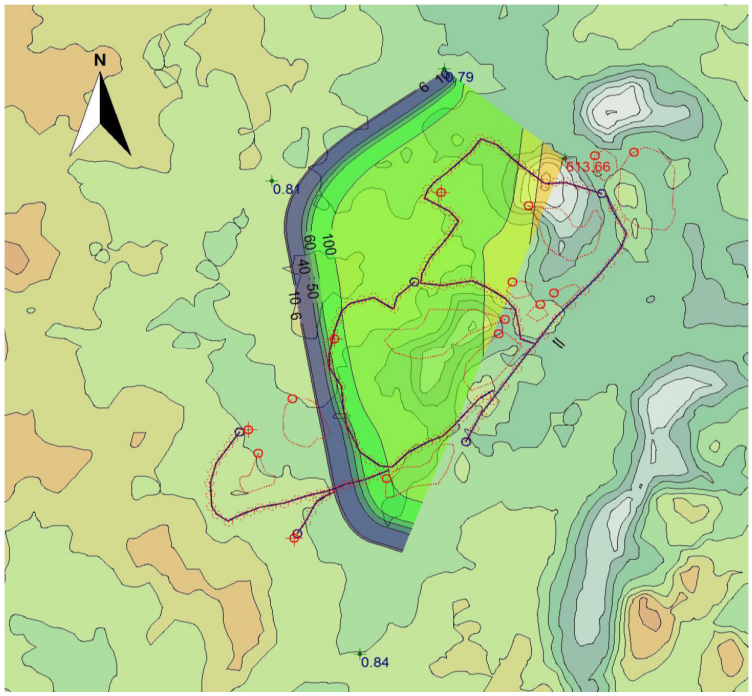

Figure 3.27:22nd Highest predicted concentration level of PM_{10} with inbuilt values for daily averaging time period in January 2013

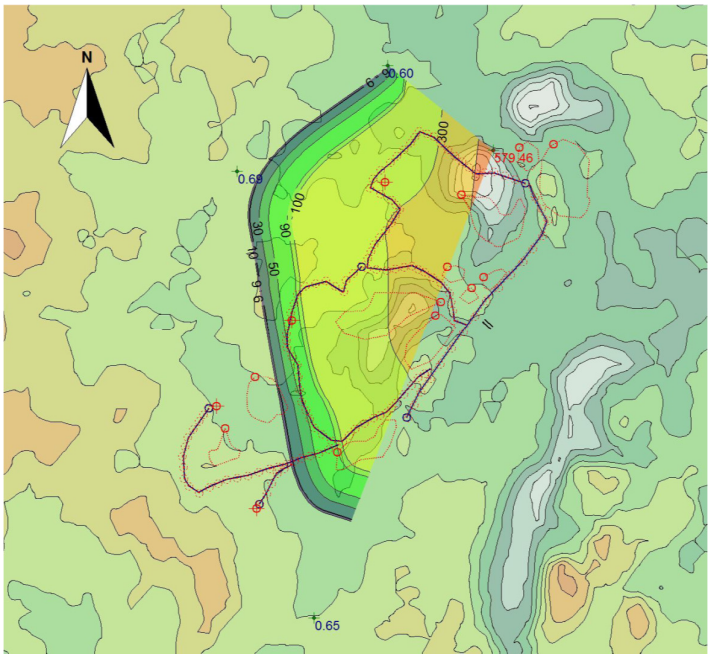

Figure 3.28:23rd Highest predicted concentration level of PM_{10} with inbuilt values for daily averaging time period in January 2013

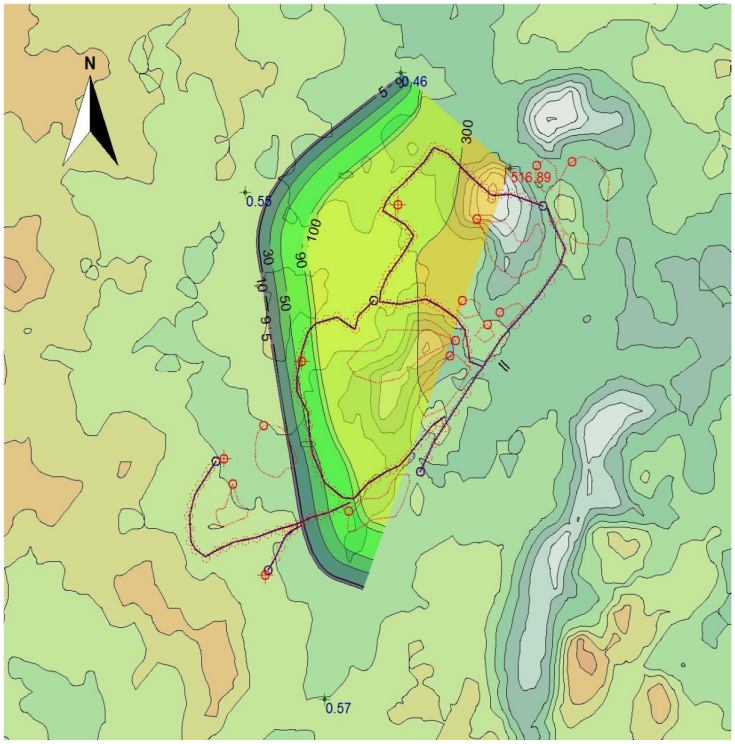

Figure 3.29:24th Highest predicted concentration level of PM_{10} with inbuilt values for daily averaging time period in January 2013

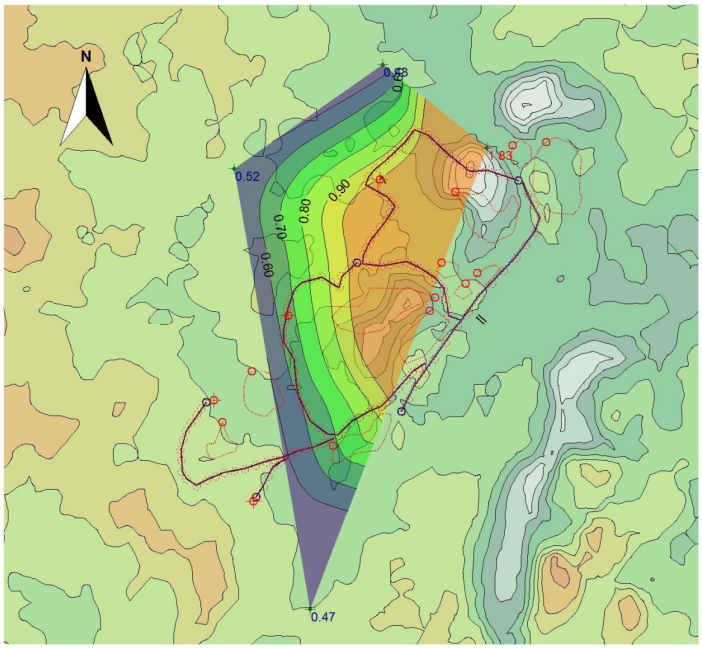

Figure 3.30:25th Highest predicted concentration level of PM_{10} with inbuilt values for daily averaging time period in January 2013

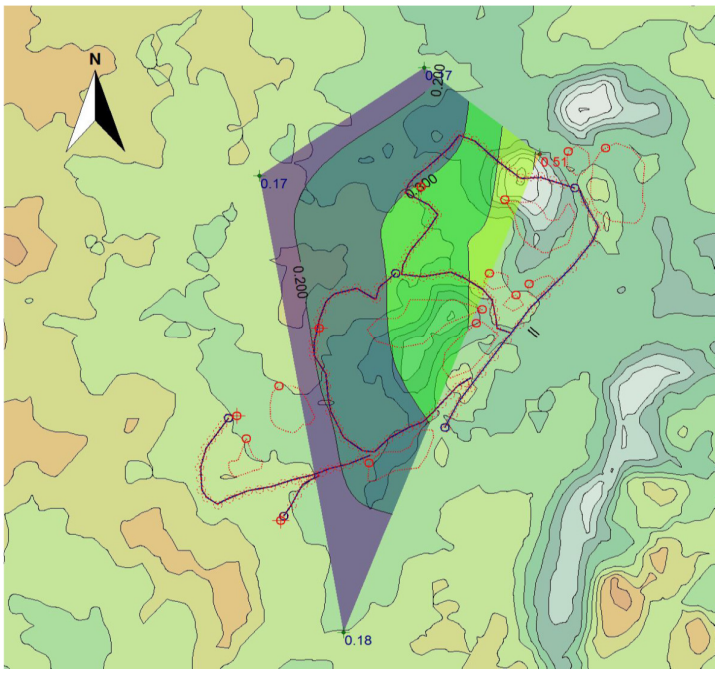

Figure 3.31: 26th Highest predicted concentration level of PM_{10} with inbuilt values for daily averaging time period in January 2013

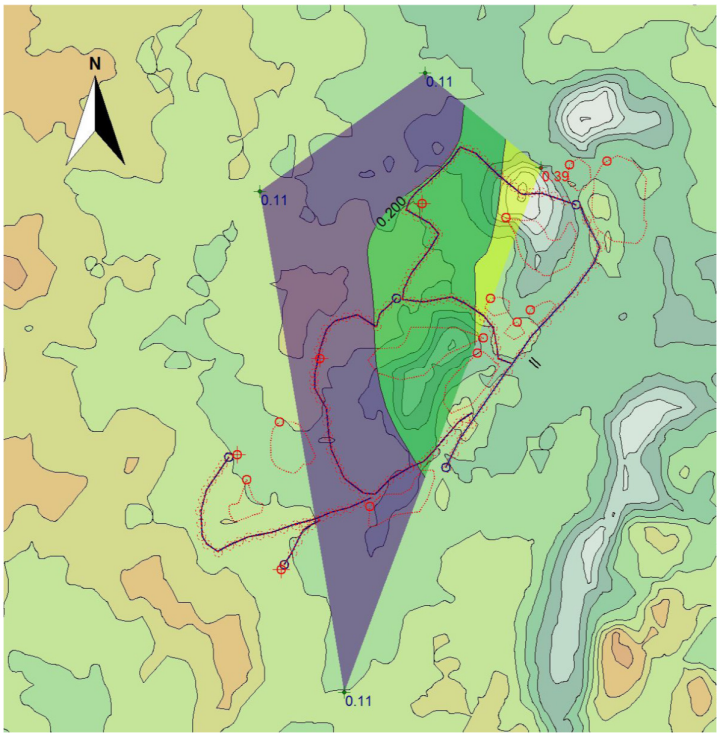

Figure 3.32: 27th Highest predicted concentration level of PM_{10} with inbuilt values for daily averaging time period in January 2013

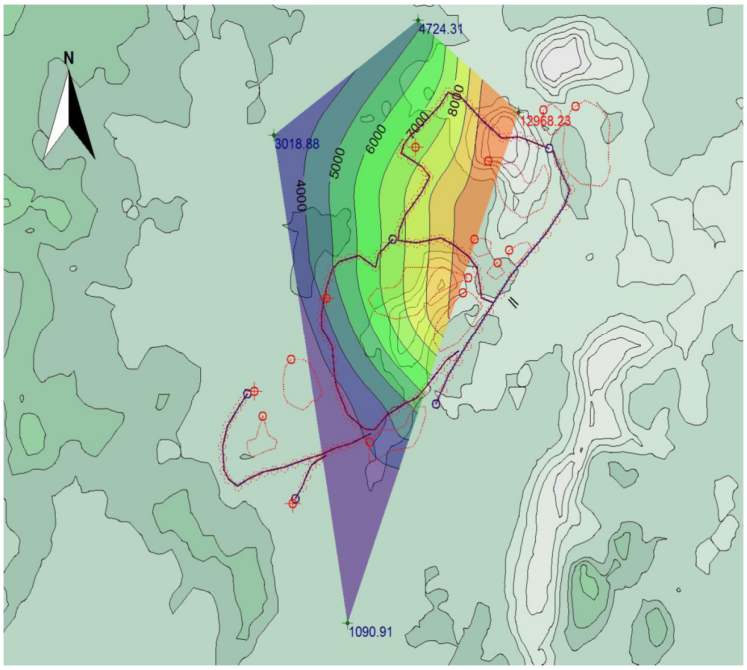

Figure 3.33: 1st Highest predicted concentration level of PM_{10} with inbuilt values for daily averaging time period in May 2013

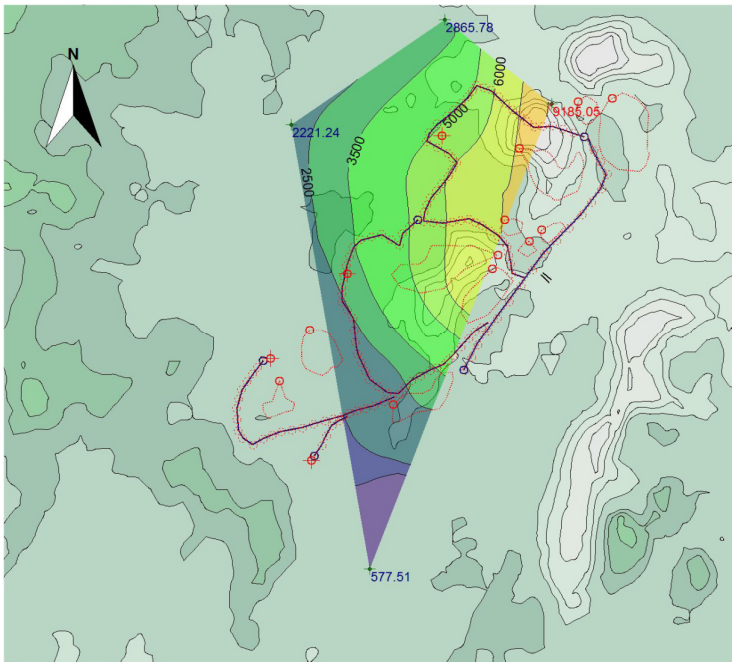

Figure 3.34: 2nd Highest predicted concentration level of PM_{10} with inbuilt values for daily averaging time period in May 2013

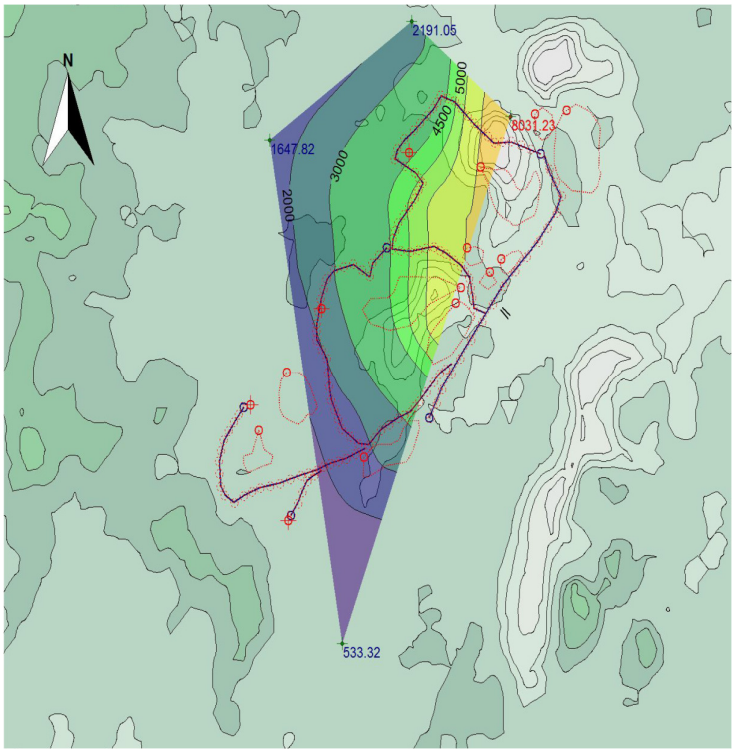

Figure 3.35: 3rd Highest predicted concentration level of PM_{10} with inbuilt values for daily averaging time period in May 2013

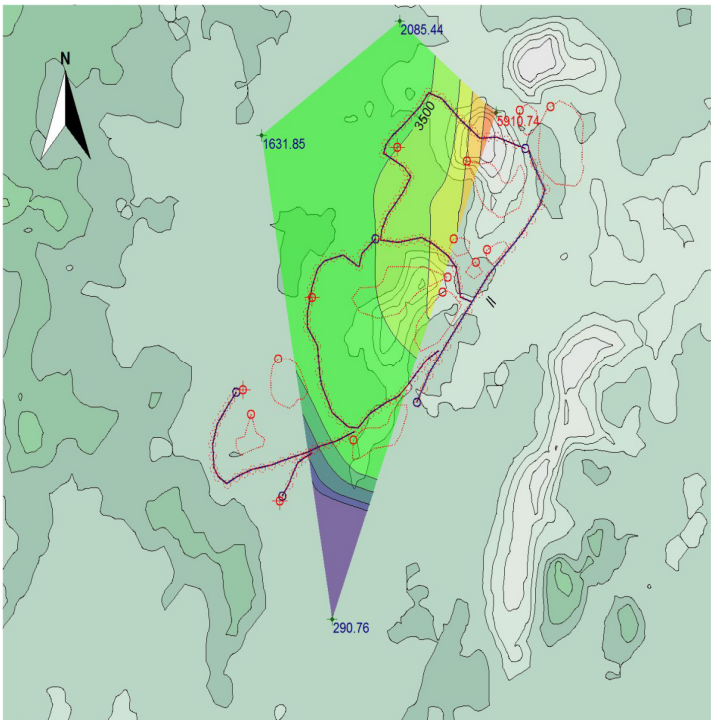

Figure 3.36: 4th Highest predicted concentration level of PM_{10} with inbuilt values for daily averaging time period in May 2013

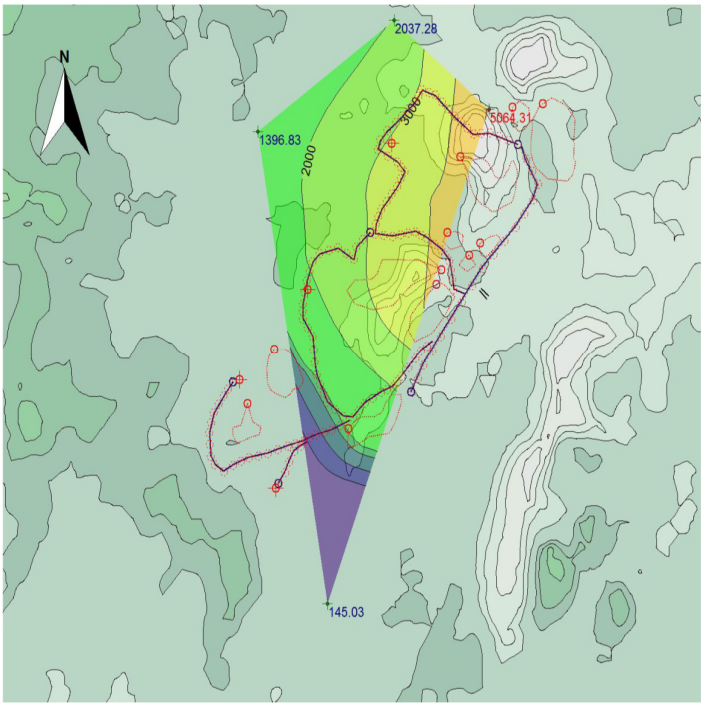

Figure 3.37: 5th Highest predicted concentration level of PM_{10} with inbuilt values for daily averaging time period in May 2013

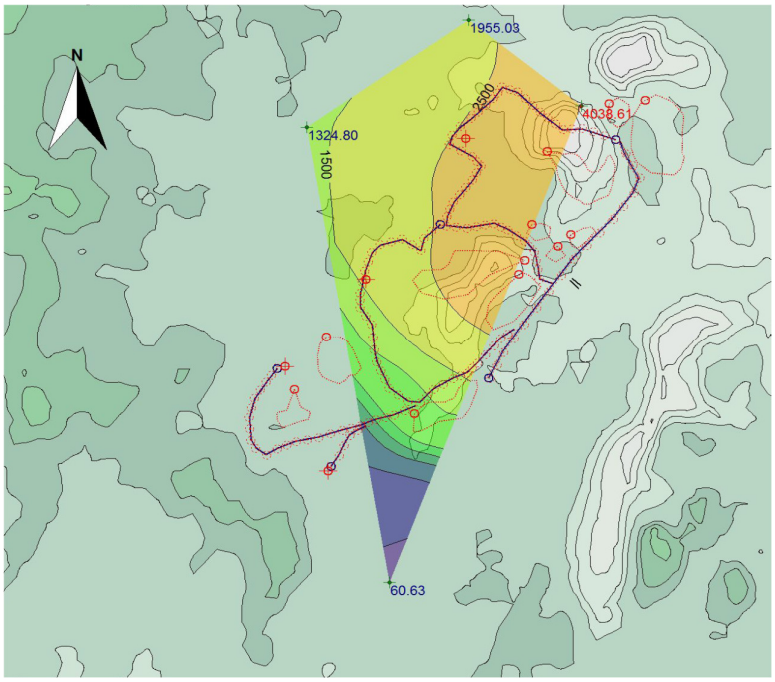

Figure 3.38: 6th Highest predicted concentration level of PM_{10} with inbuilt values for daily averaging time period in May 2013

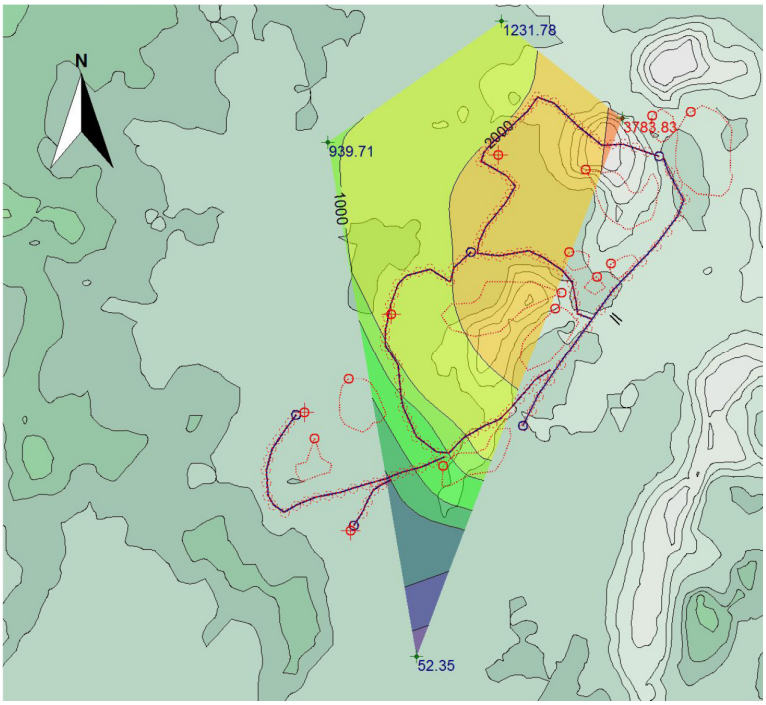

Figure 3.39: 7th Highest predicted concentration level of PM_{10} with inbuilt values for daily averaging time period in May 2013

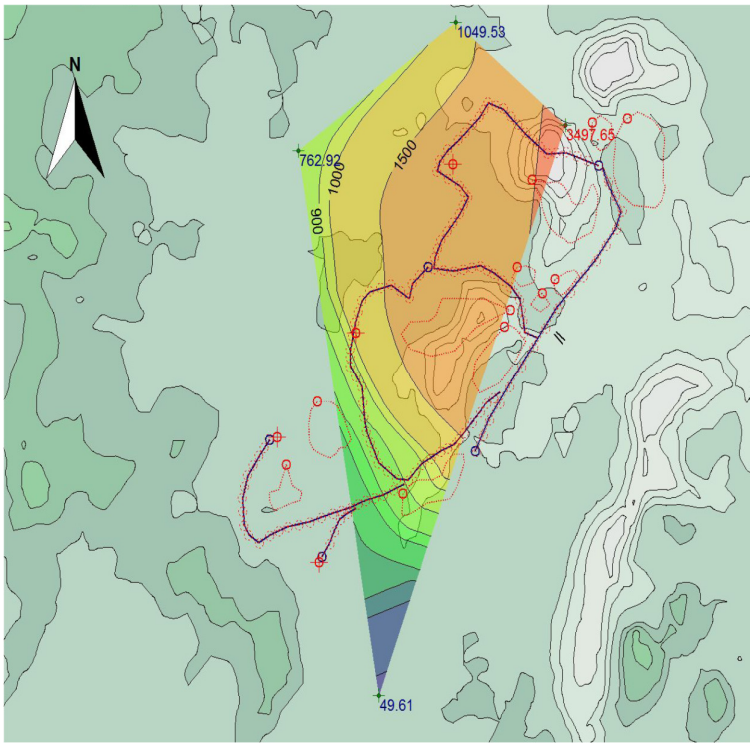

Figure 3.40: 8th Highest predicted concentration level of PM_{10} with inbuilt values for daily averaging time period in May 2013

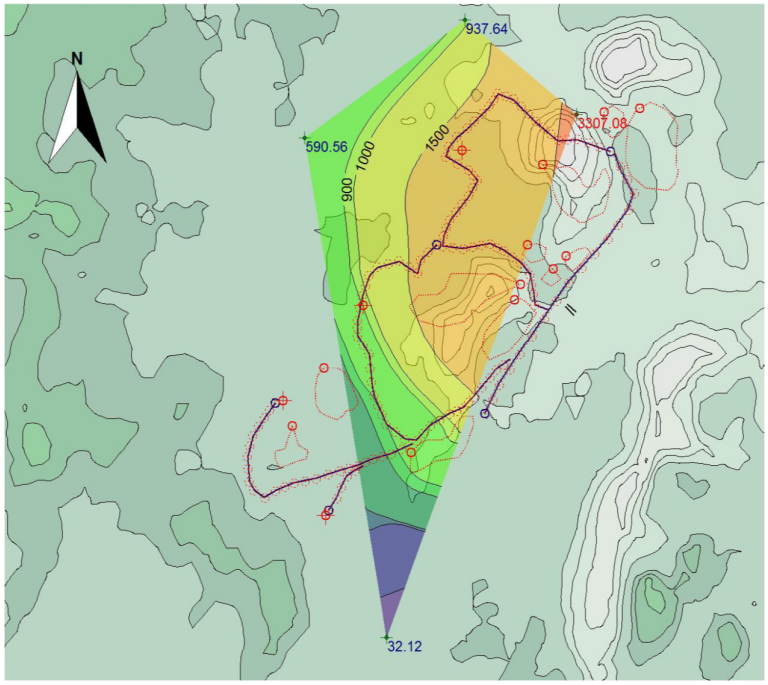

Figure 3.41: 9th Highest predicted concentration level of PM_{10} with inbuilt values for daily averaging time period in May 2013

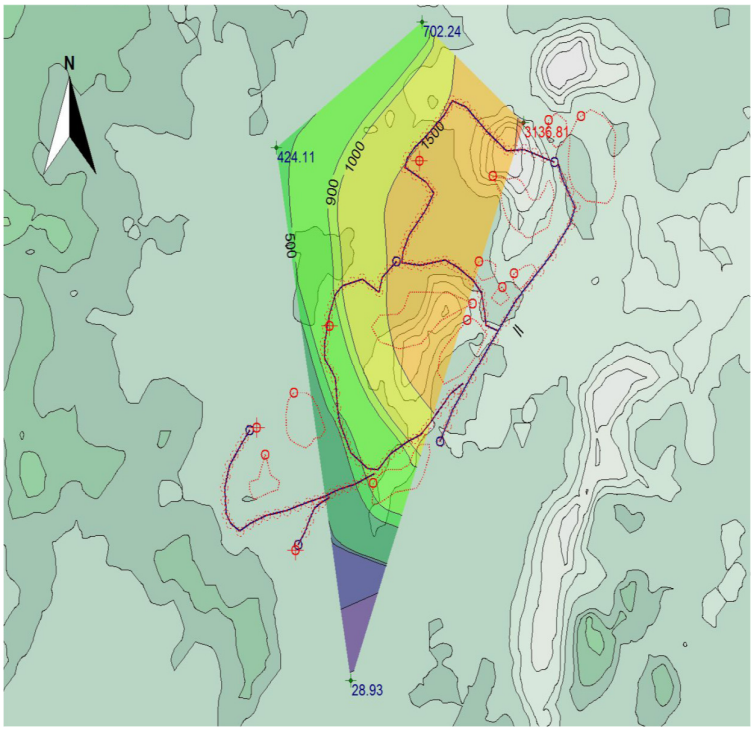

Figure 3.42: 10th Highest predicted concentration level of PM_{10} with inbuilt values for daily averaging time period in May 2013

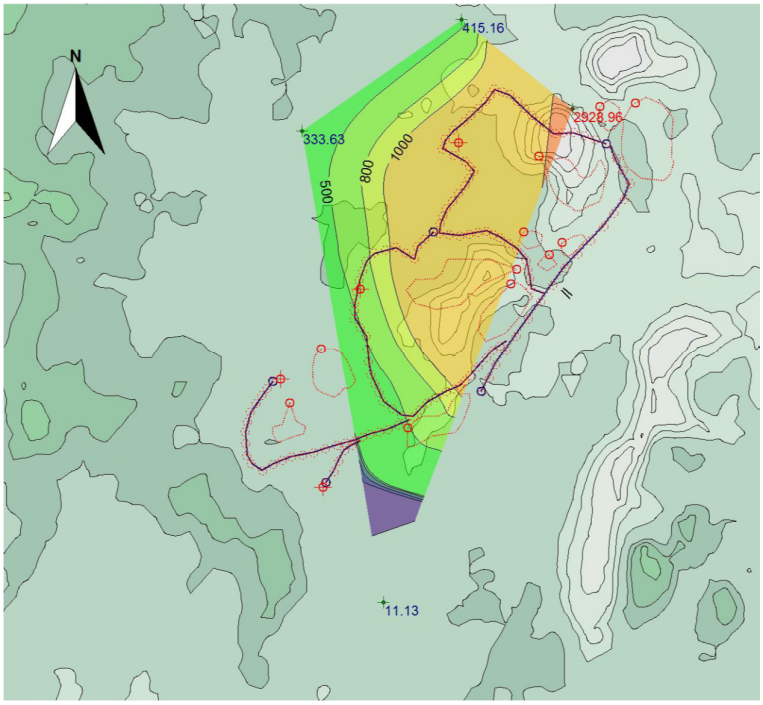

Figure 3.43: 11th Highest predicted concentration level of PM_{10} with inbuilt values for daily averaging time period in May 2013

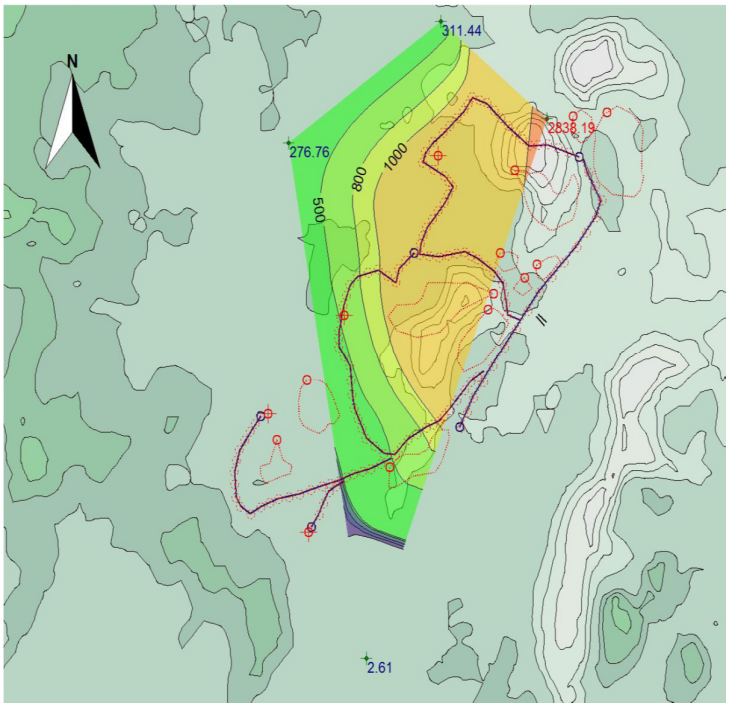

Figure 3.44: 12th Highest predicted concentration level of PM_{10} with inbuilt values for daily averaging time period in May 2013

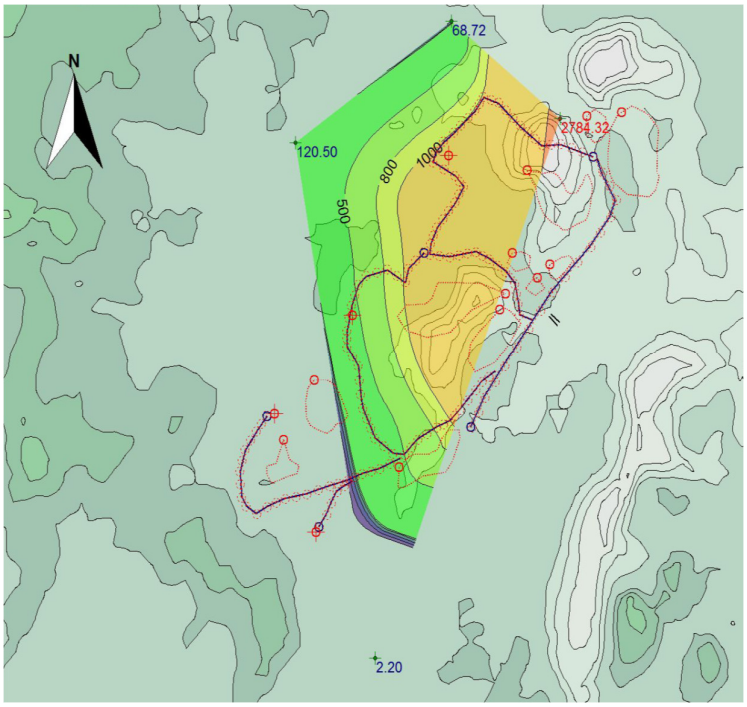

Figure 3.45: 13th Highest predicted concentration level of PM_{10} with inbuilt values for daily averaging time period in May 2013

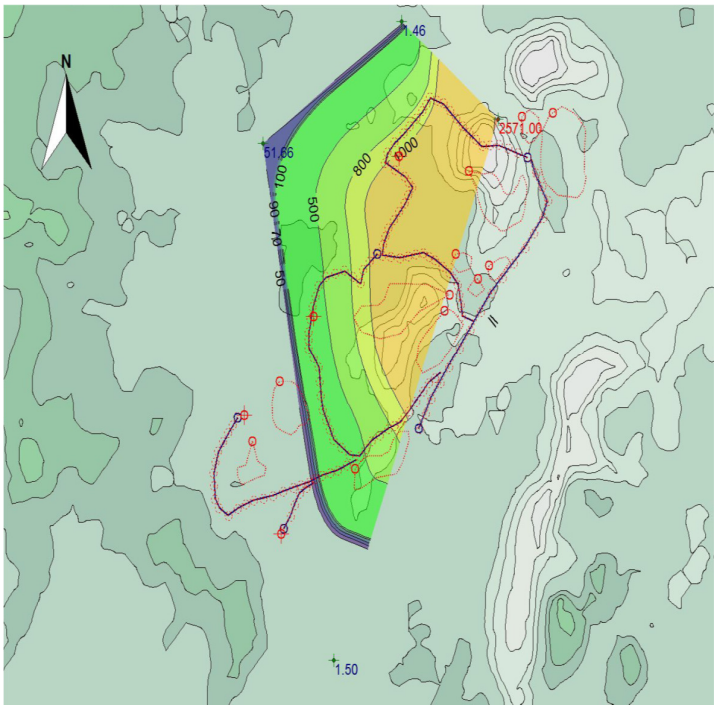

Figure 3.46: 14th Highest predicted concentration level of PM_{10} with inbuilt values for daily averaging time period in May 2013

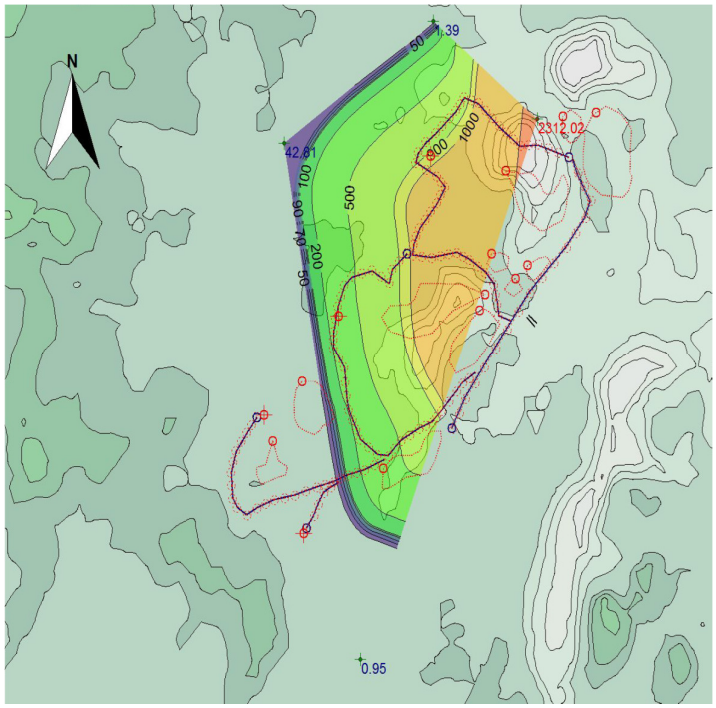

Figure 3.47: 15th Highest predicted concentration level of PM_{10} with inbuilt values for daily averaging time period in May 2013

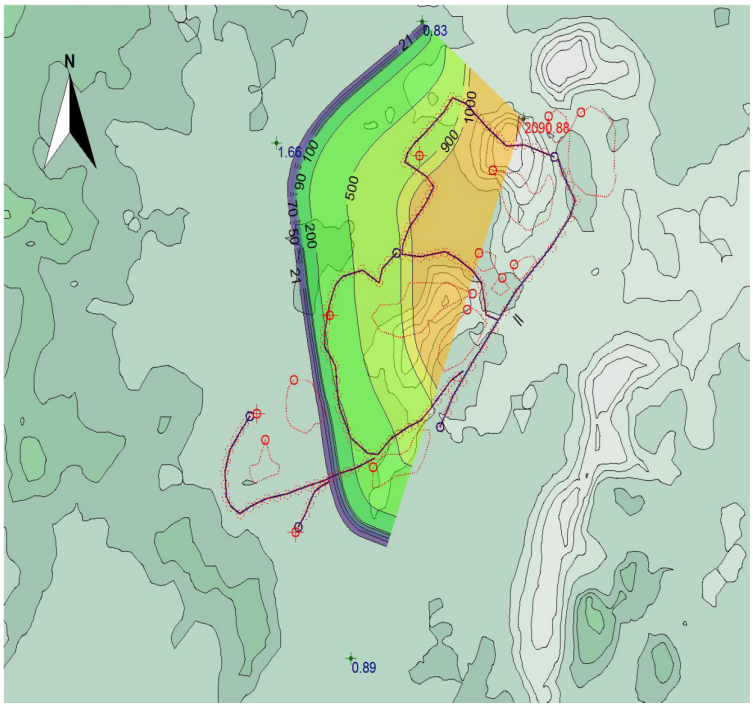

Figure 3.48: 16th Highest predicted concentration level of PM_{10} with inbuilt values for daily averaging time period in May 2013

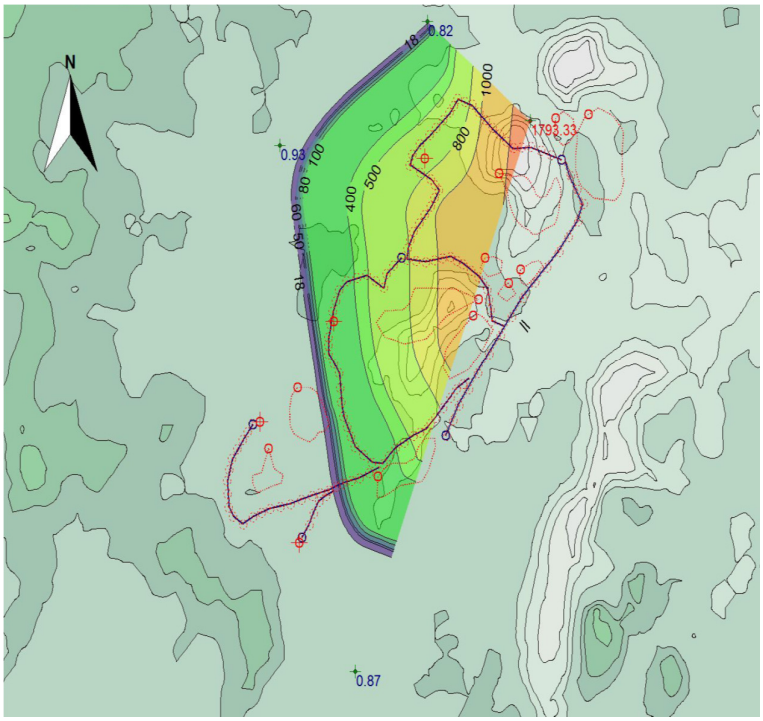

Figure 3.49: 17th Highest predicted concentration level of PM_{10} with inbuilt values for daily averaging time period in May 2013

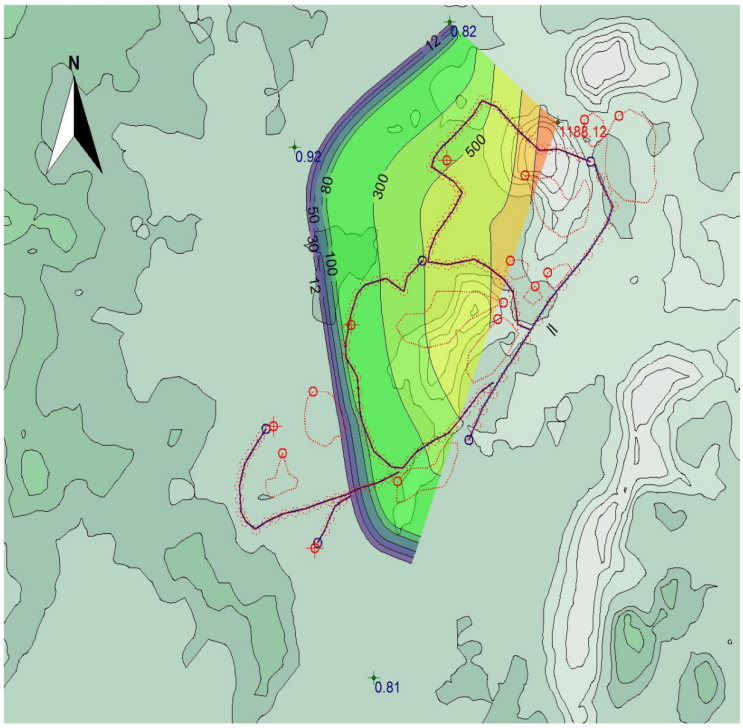

Figure 3.50: 18th Highest predicted concentration level of PM_{10} with inbuilt values for daily averaging time period in May 2013

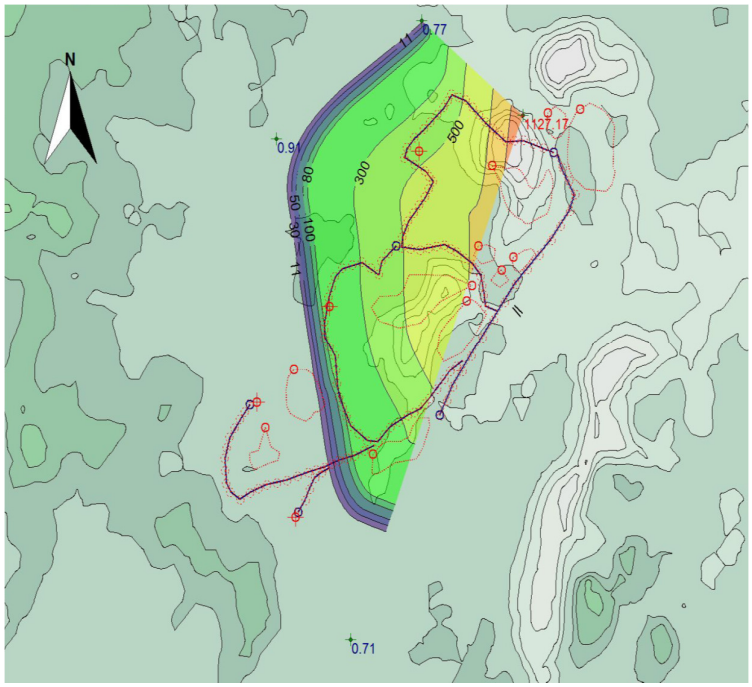

Figure 3.51: 19th Highest predicted concentration level of PM_{10} with inbuilt values for daily averaging time period in May 2013

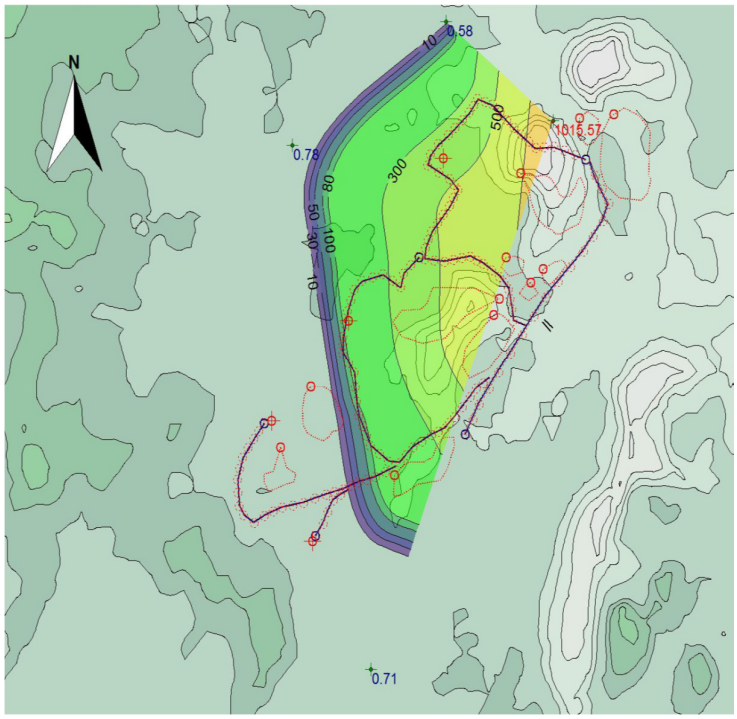

Figure 3.52:20th Highest predicted concentration level of PM_{10} with inbuilt values for daily averaging time period in May 2013

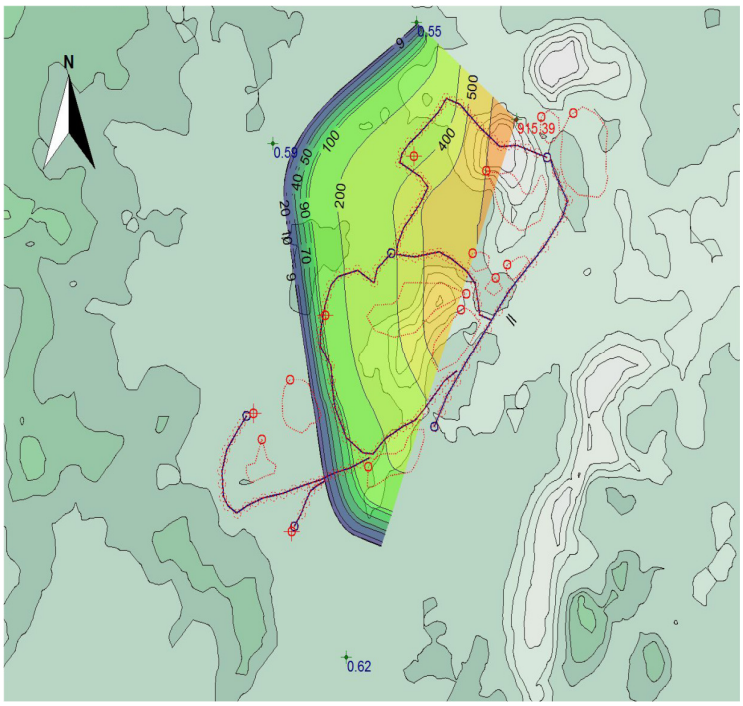

Figure 3.53:21st Highest predicted concentration level of PM_{10} with inbuilt values for daily averaging time period in May 2013

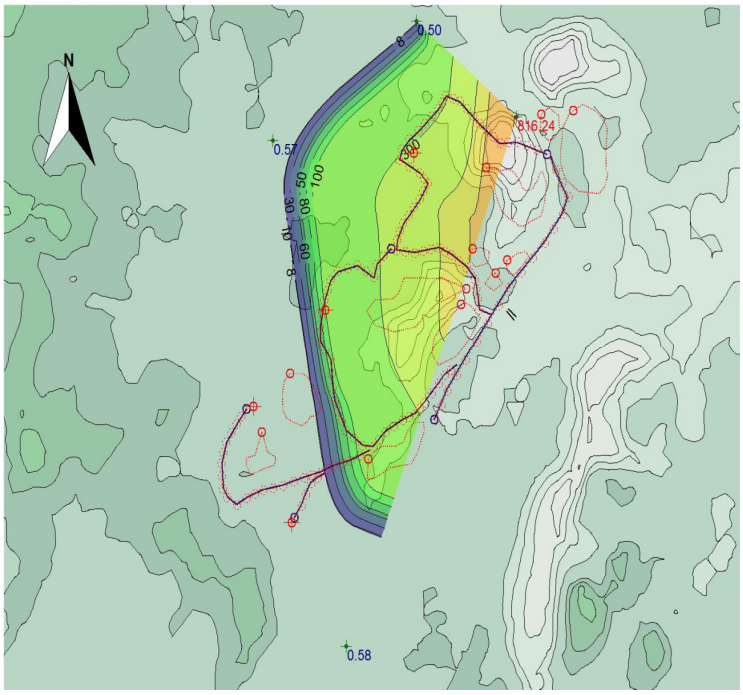

Figure 3.54:22nd Highest predicted concentration level of PM_{10} with inbuilt values for daily averaging time period in May 2013

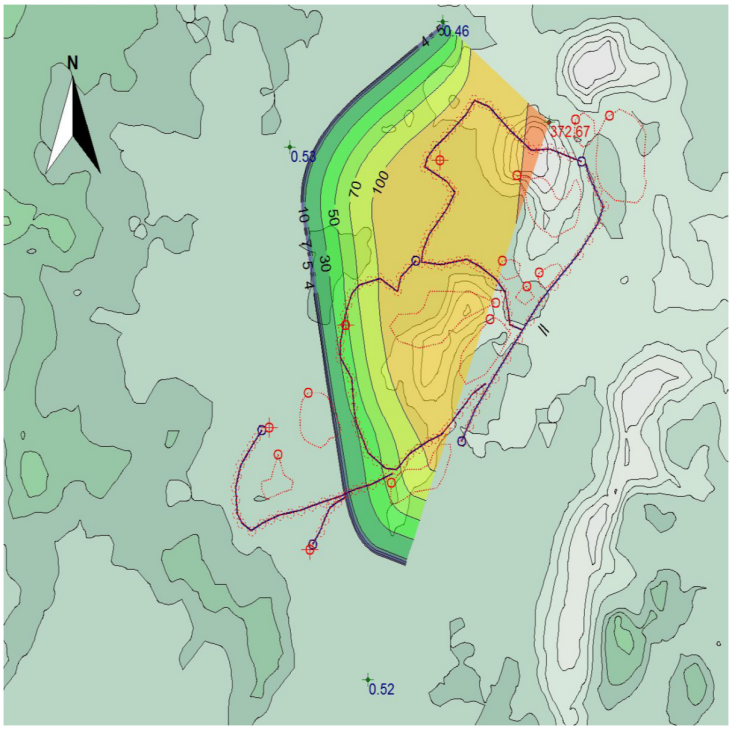

Figure 3.55:23rd Highest predicted concentration level of PM_{10} with inbuilt values for daily averaging time period in May 2013

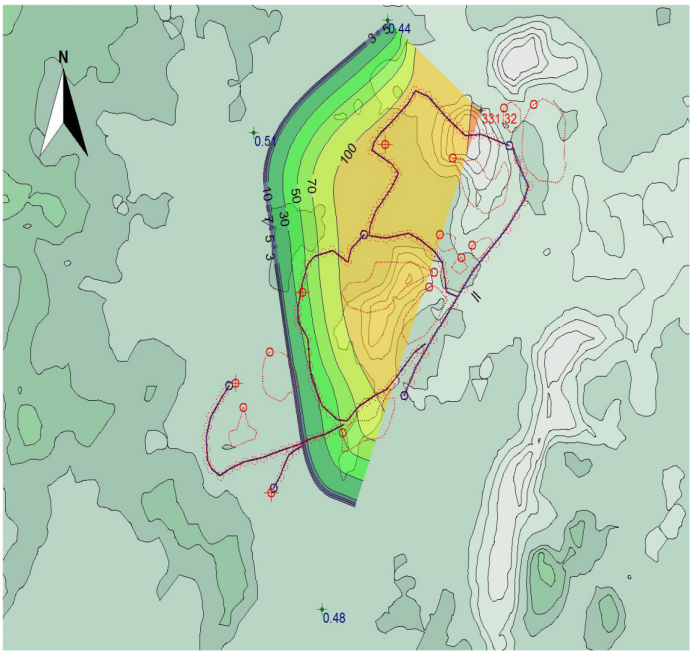

Figure 3.56: 24th Highest predicted concentration level of PM_{10} with inbuilt values for daily averaging time period in May 2013

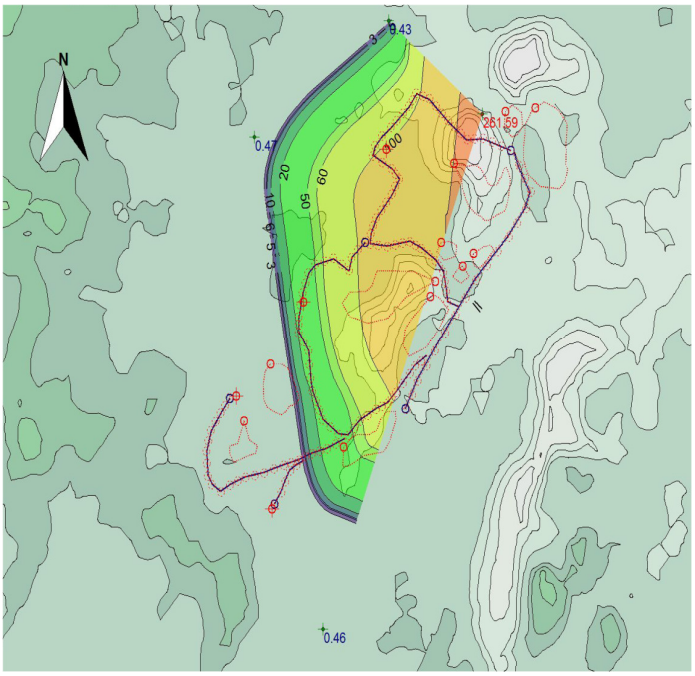

Figure 3.57: 25th Highest predicted concentration level of PM_{10} with inbuilt values for daily averaging time period in May 2013

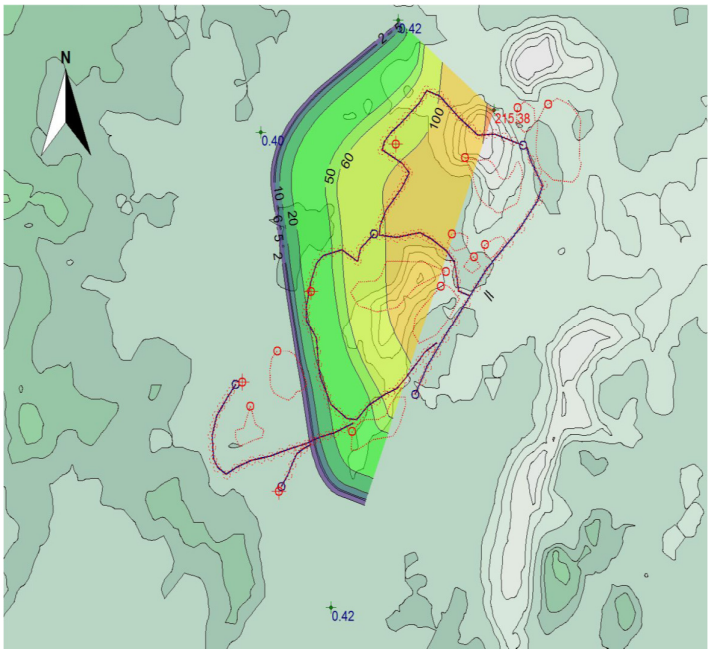

Figure 3.58: 26th Highest predicted concentration level of PM_{10} with inbuilt values for daily averaging time period in May 2013

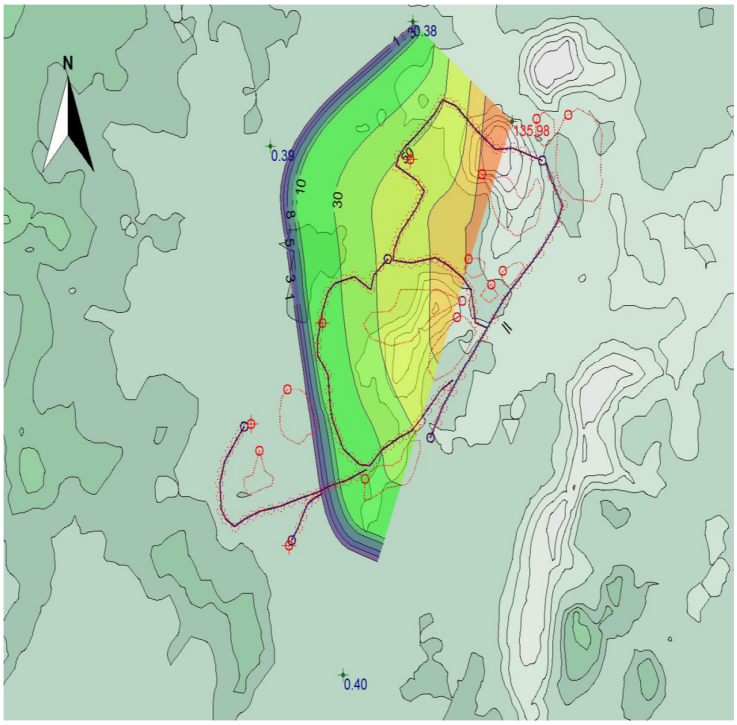

Figure 3.59: 27th Highest predicted concentration level of PM_{10} with inbuilt values for daily averaging time period in May 2013

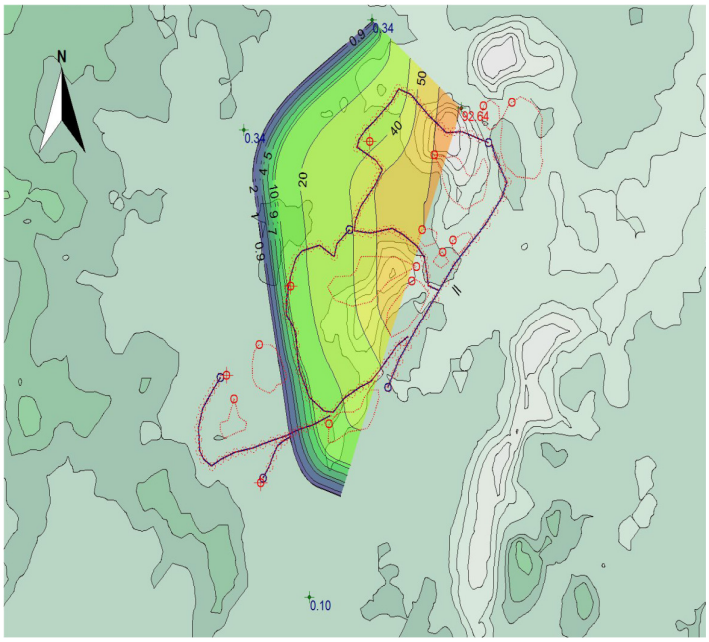

Figure 3.60: 28th Highest predicted concentration level of PM_{10} with inbuilt values for daily averaging time period in May 2013

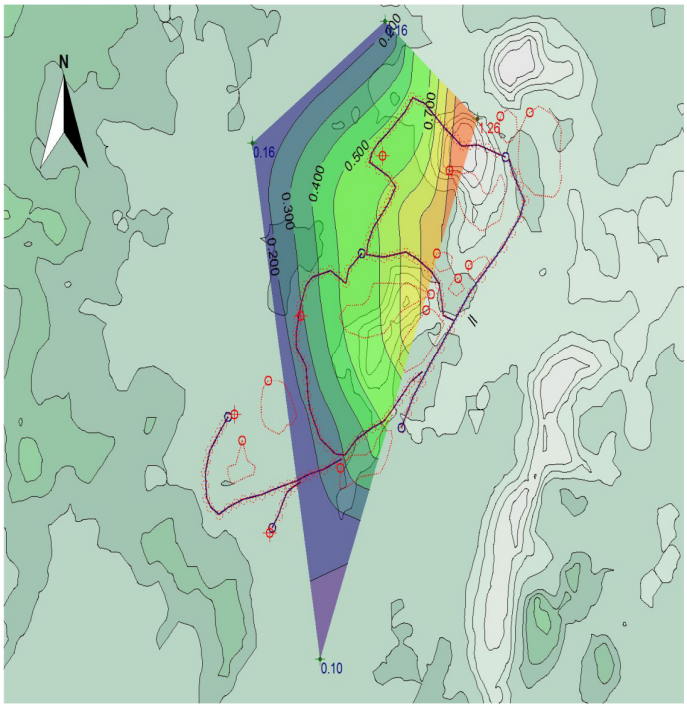

Figure 3.61: 29th Highest predicted concentration level of PM_{10} with inbuilt values for daily averaging time period in May 2013

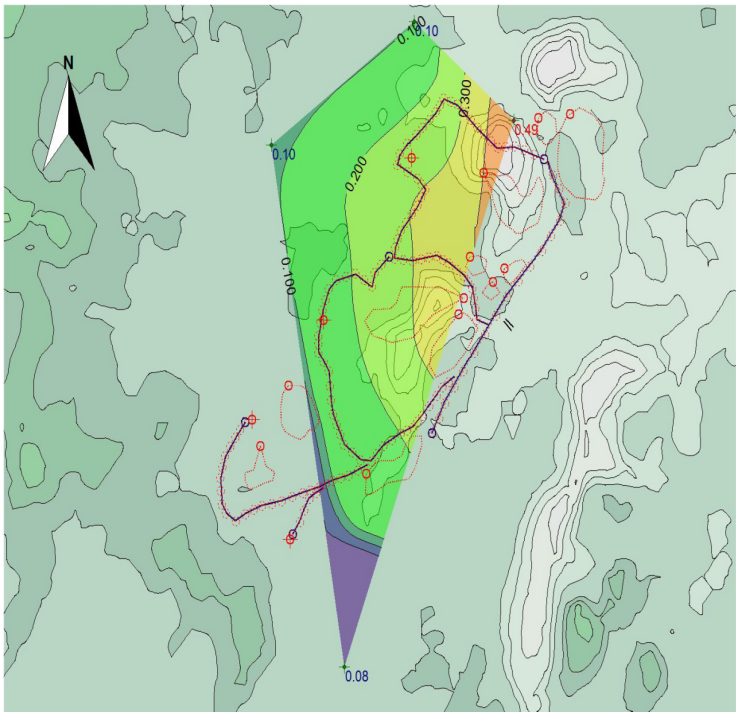

Figure 3.62: 30th Highest predicted concentration level of PM_{10} with inbuilt values for daily averaging time period in May 2013

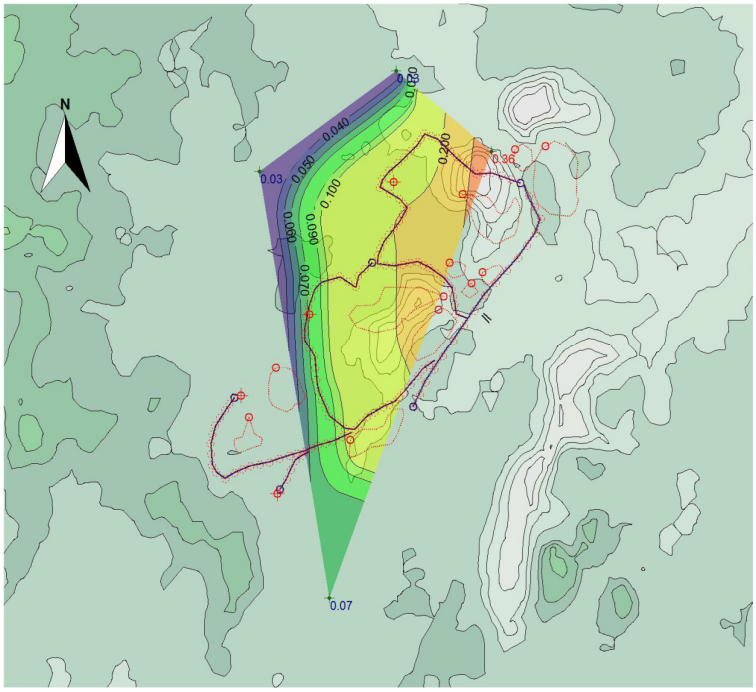

Figure 3.63: 31st Highest predicted concentration level of PM_{10} with inbuilt values for daily averaging time period in May 2013

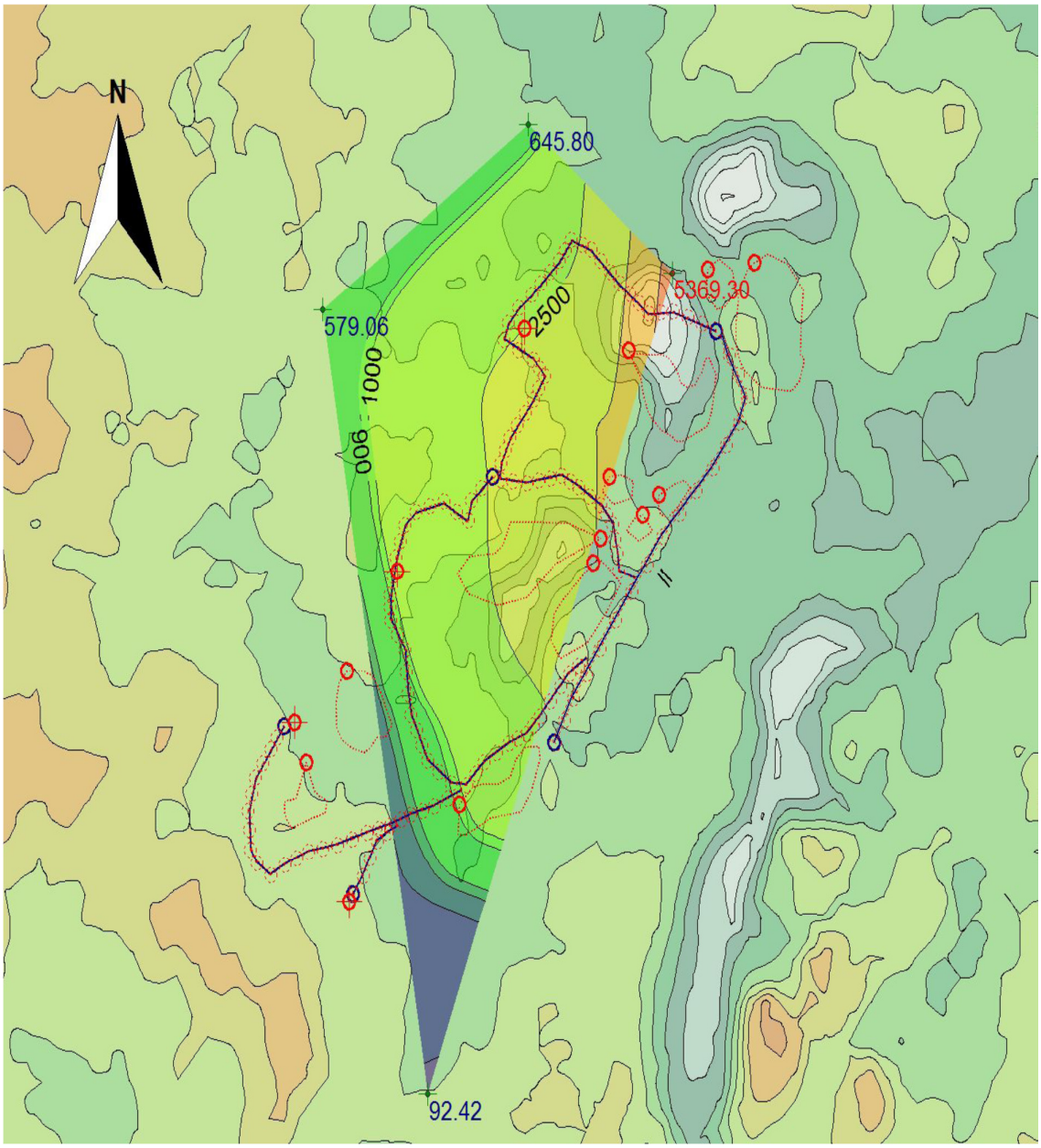

Figure 3.64: Predicted concentration level of PM_{10} with inbuilt values for monthly averaging time period in the month of January 2013

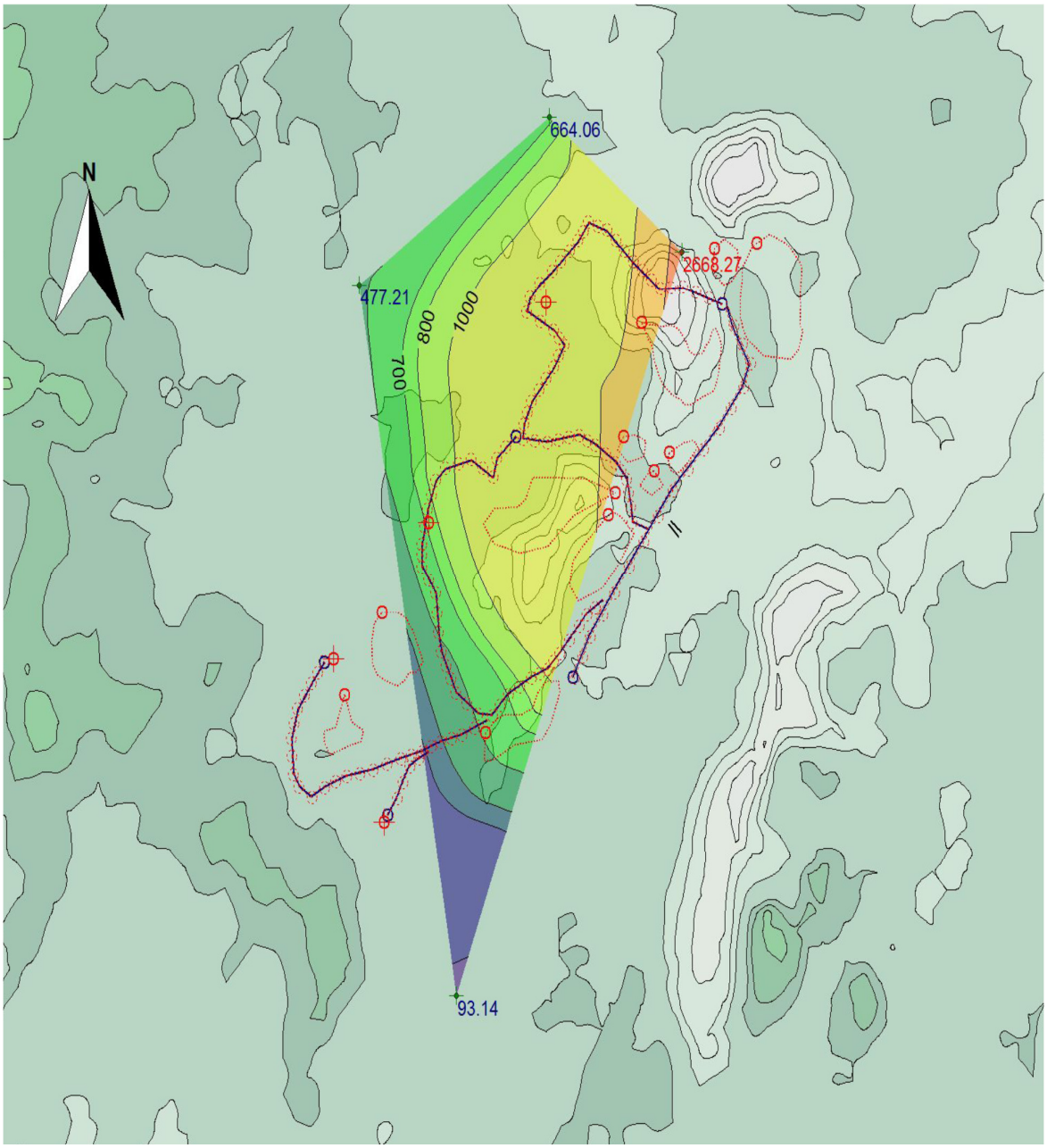

Figure 3.65: Predicted concentration level of PM_{10} with inbuilt values for monthly averaging time period in the month of May 2013

Table 3.5: Predicted daily average concentration of PM_{10} at the four receptors in µg/m^3 for January 2013

S. No.	Date	A1	Date	A2	Date	A3	Date	A4
1.	14-01-13	22866.48	17-01-13	5877.139	10-01-13	899.7112	14-01-13	5754.912
2.	17-01-13	19566.12	14-01-13	5812.667	13-01-13	832.7205	17-01-13	4570.739
3.	25-01-13	15837.4	29-01-13	4089.478	09-01-13	785.5666	25-01-13	2492.455
4.	29-01-13	15619.03	25-01-13	3146.018	11-01-13	197.1059	18-01-13	1427.903
5.	26-01-13	12724.21	18-01-13	698.509	23-01-13	97.00536	13-01-13	1206.83
6.	09-01-13	11429.16	20-01-13	344.5221	14-01-13	7.02585	01-01-13	1178.98
7.	10-01-13	9589.616	09-01-13	6.53373	26-01-13	6.94144	29-01-13	804.8265
8.	11-01-13	8859.296	13-01-13	6.49396	29-01-13	6.37421	20-01-13	279.6798
9.	13-01-13	8639.83	26-01-13	6.40248	25-01-13	4.59135	12-01-13	188.3433
10.	12-01-13	8196.572	10-01-13	5.64132	28-01-13	4.15588	29-01-13	7.90019
11.	15-01-13	7299.136	11-01-13	4.26001	12-01-13	3.95264	26-01-13	7.73638
12.	28-01-13	6423.1	28-01-13	3.86333	17-01-13	3.89947	10-01-13	6.81997
13.	08-01-13	3838.353	12-01-13	3.66206	15-01-13	3.23871	11-01-13	5.08692
14.	19-01-13	3111.253	15-01-13	2.99824	01-01-13	2.34375	28-01-13	4.64875
15.	18-01-13	2930.321	01-01-13	2.16093	22-01-13	1.76977	15-01-13	3.54749
16.	20-01-13	2254.81	22-01-13	1.63714	02-01-13	1.54971	22-01-13	1.97501
17.	30-01-13	1651.663	02-01-13	1.44511	08-01-13	0.9152	02-01-13	1.63734
18.	22-01-13	1549.923	08-01-13	0.87946	27-01-13	0.88164	30-01-13	0.96164
19.	27-01-13	886.9965	27-01-13	0.8239	18-01-13	0.86052	27-01-13	0.92166
20.	31-01-13	811.7092	19-01-13	0.8013	30-01-13	0.86024	08-01-13	0.88494
21.	02-01-13	659.5	30-01-13	0.79832	31-01-13	0.84616	31-01-13	0.88482
22.	16-01-13	613.7016	31-01-13	0.79374	19-01-13	0.84175	19-01-13	0.81306
23.	21-01-13	579.4576	07-01-13	0.60455	07-01-13	0.64828	07-01-13	0.69419
24.	03-01-13	516.8881	23-01-13	0.45617	20-01-13	0.57036	23-01-13	0.5469
25.	01-01-13	1.82588	16-01-13	0.43318	16-01-13	0.4699	16-01-13	0.52351
26.	07-01-13	0.51201	21-01-13	0.16749	21-01-13	0.17607	21-01-13	0.17098
27.	23-01-13	0.38591	03-01-13	0.10564	03-01-13	0.11095	03-01-13	0.10798

Table 3.6: Predicted daily average concentration of PM_{10} at the four receptors in µg/m^3 for May 2013

S. No.	Date	A1	Date	A2	Date	A3	Date	A4
1.	13-05-13	12968.23	13-05-13	4724.308	15-05-13	1090.915	13-05-13	3018.875
2.	14-05-13	9185.048	14-05-13	2865.783	04-05-13	577.5097	14-05-13	2221.237
3.	09-05-13	8031.232	31-05-13	2191.055	29-05-13	533.3212	26-05-13	1647.825
4.	31-05-13	5910.744	26-05-13	2085.44	17-05-13	290.763	31-05-13	1631.849
5.	26-05-13	5064.312	09-05-13	2037.28	11-05-13	145.0334	16-05-13	1396.825
6.	27-05-13	4038.61	27-05-13	1955.03	21-05-13	60.62563	15-05-13	1324.804
7.	12-05-13	3783.827	12-05-13	1231.781	19-05-13	52.34832	12-05-13	939.711
8.	10-05-13	3497.645	24-05-13	1049.53	20-05-13	49.60694	18-05-13	762.9158
9.	01-05-13	3307.075	10-05-13	937.6441	06-05-13	32.11758	28-05-13	590.563
10.	08-05-13	3136.808	28-05-13	702.2398	14-05-13	28.93322	24-05-13	424.1074
11.	23-05-13	2928.955	03-05-13	415.1636	07-05-13	11.1328	27-05-13	333.6303
12.	05-05-13	2838.192	16-05-13	311.4365	09-05-13	2.608	09-05-13	276.757
13.	19-05-13	2784.316	02-05-13	68.71662	26-05-13	2.19919	10-05-13	120.5015
14.	06-05-13	2571.004	15-05-13	1.46232	25-05-13	1.50485	03-05-13	51.66131
15.	22-05-13	2312.019	25-05-13	1.39047	13-05-13	0.94937	02-05-13	42.81389
16.	28-05-13	2090.883	08-05-13	0.83433	08-05-13	0.89162	25-05-13	1.66229
17.	24-05-13	1793.334	19-05-13	0.81969	22-05-13	0.87318	08-05-13	0.93232
18.	04-05-13	1188.119	22-05-13	0.81646	01-05-13	0.80551	19-05-13	0.9174
19.	03-05-13	1127.168	01-05-13	0.76538	31-05-13	0.71049	22-05-13	0.9131
20.	07-05-13	1015.571	29-05-13	0.57789	28-05-13	0.70901	01-05-13	0.77899
21.	02-05-13	915.3899	23-05-13	0.55498	27-05-13	0.61652	29-05-13	0.58773
22.	20-05-13	816.2406	06-05-13	0.50396	23-05-13	0.58379	23-05-13	0.56562
23.	16-05-13	372.6679	05-05-13	0.46112	10-05-13	0.52183	20-05-13	0.53191
24.	25-05-13	331.3206	20-05-13	0.44154	05-05-13	0.48492	06-05-13	0.51351

25.	30-05-13	261.5873	18-05-13	0.42791	18-05-13	0.46367	05-05-13	0.47041
26.	17-05-13	215.3766	11-05-13	0.41732	16-05-13	0.41575	11-05-13	0.40476
27.	21-05-13	135.9819	30-05-13	0.3846	30-05-13	0.40485	30-05-13	0.39117
28.	11-05-13	92.63861	04-05-13	0.33838	24-05-13	0.10162	04-05-13	0.34393
29.	15-05-13	1.25665	07-05-13	0.15596	02-05-13	0.09619	07-05-13	0.15963
30.	29-05-13	0.49342	17-05-13	0.09676	12-05-13	0.07663	17-05-13	0.09909
31.	18-05-13	0.3613	21-05-13	0.02594	03-05-13	0.06526	21-05-13	0.02691

Table 3.7: Predicted monthly average concentration of PM_{10} at the four receptors in $\mu g/m^3$ for January and May of 2013

Month	A1	A2	A3	A4
1.	5369.588	645.7837	92.42366	579.0493
2.	2668.27	664.06	93.14	477.21

3.5. Measurement of concentration of PM_{10} at different locations (receptors) of High Volume Samplers

Ambient fine dust samplers (Make: Instrumex, Model No. IPM-FDS) installed at locations, namely A1, A2, A3 & A4 had measured concentration of PM_{10} on daily basis. These dust samplers are having arrangement to measure $PM_{.5}$ along with PM_{10}. WINS impactor assembly has been removed to take only PM_{10} measurement. A 47 mm glass fibre filter paper has been used to measure the daily concentration of PM_{10} at all four receptors. All the filter papers were dried out in an oven and then used for the sampling. These fine dust samplers had been usually started at 8:00 hrs in the morning. Next day, around 7:45 hrs in the morning, these filters papers were removed and new one were used to placed. The difference between the final weight and initial weight of the filter paper had provided the PM_{10} deposition for the whole day. These samplers are designed at a flow rate of $1m^3$/hr with the help of a micro-processor. Flow rate was multiplied with the total duration in a day for which the fine dust sampler had run. This had given the total volume of the air sampled. The ratio of the dust deposited on the filter paper and volume of the air sampled had provide the concentration of PM_{10} for the particular day.

The measurements made at different receptors for 24 hour (daily) averaging period of PM_{10} concentrations have been summarised in Table 3.8 for the month of January 2013 and Table 3.9 for the month of May 2013. Similarly these measurements were also carried out for the monthly averaging time period and these are shown in Table 3.10 for the month of January and May of 2013.

Table 3.8: Measured concentration of PM_{10} at different receptors (A1, A2, A3, A4) in the month of January 2013 for 24 hr averaging time period in µg/m^3

S. No.	Date	A1	A2	A3	A4
1.	01-01-2013	2.89	2.2	3.33	1192
2.	02-01-2013	728	1.48	1.22	2.07
3.	03-01-2013	505	0.22	0.22	0.27
4.	04-01-2013	0.89	0.16	0.12	0.27
5.	05-01-2013	0.96	0.12	0.19	0.11
6.	06-01-2013	0.89	0.15	0.11	0.13
7.	07-01-2013	1.17	0.73	0.46	0.7
8.	08-01-2013	3564	0.92	1.18	0.82
9.	09-01-2013	10985	7.28	430	6.82
10.	10-01-2013	9352	6.01	760	5.88
11.	11-01-2013	8256	4.82	120	220
12.	12-01-2013	8009	3.12	4.18	1228
13.	13-01-2013	8146	6.99	670	5240
14.	14-01-2013	18460	4860	85	3.82

15.	15-01-2013	7521	3.03	3.52	0.55
16.	16-01-2013	690	0.25	0.38	4520
17.	17-01-2013	17230	5450	3.74	1240
18.	18-01-2013	3000	721	0.82	0.72
19.	19-01-2013	3274	0.83	0.7	312
20.	20-01-2013	2447	319	0.41	0.53
21.	21-01-2013	523	0.23	0.27	2.23
22.	22-01-2013	1680	1.58	2.17	0.58
23.	23-01-2013	1.03	0.68	118	0.11
24.	24-01-2013	0.37	0.18	0.11	2120
25.	25-01-2013	16558	2280	5.22	7.11
26.	26-01-2013	11100	6.42	10.23	0.87
27.	27-01-2013	1550	0.87	0.89	5.03
28.	28-01-2013	6822	3.24	5.03	728
29.	29-01-2013	12560	3620	6.88	10.89
30.	30-01-2013	1722	0.76	0.76	0.89
31.	31-01-2013	1097	0.73	0.73	0.73

Table 3.9: Measured concentration of PM_{10} at different receptors in the month of May 2013 for 24 hr averaging time in µg/m^3

S. No.	**Date**	**A1**	**A2**	**A3**	**A4**
1.	01-05-2013	3266	0.72	0.8	0.83
2.	02-05-2013	903	62	0.12	42.1
3.	03-05-2013	1120	463	0.09	53.2
4.	04-05-2013	1203	0.32	455	0.28
5.	05-05-2013	2943	0.48	0.47	0.41
6.	06-05-2013	2618	0.52	38	0.44
7.	07-05-2013	908	0.2	9.56	0.23
8.	08-05-2013	3005	0.89	0.88	0.98
9.	09-05-2013	7290	1760	2.54	294
10.	10-05-2013	3548	940	0.51	112
11.	11-05-2013	90	0.38	150	0.38
12.	12-05-2013	3880	1157	0.1	972
13.	13-05-2013	11870	3670	0.95	2860
14.	14-05-2013	10480	3200	32.4	2160
15.	15-05-2013	1.25	1.58	860	1294
16.	16-05-2013	388	310	0.38	1408
17.	17-05-2013	219	0.09	220	0.23
18.	18-05-2013	0.44	0.41	0.42	758
19.	19-05-2013	2722	0.75	50.44	0.95
20.	20-05-2013	882	0.42	50.1	0.51
21.	21-05-2013	110	0.07	68.12	0.23
22.	22-05-2013	2310	0.77	0.83	0.92
23.	23-05-2013	3002	0.55	0.52	0.52

24.	24-05-2013	1779	1083	0.31	493
25.	25-05-2013	350	1.22	1.58	2.33
26.	26-05-2013	5033	1856	2.21	1647
27.	27-05-2013	4134	1738	0.54	367
28.	28-05-2013	2113	709	0.61	558
29.	29-05-2013	0.52	0.58	360	0.71
30.	30-05-2013	270	0.33	0.33	0.32
31.	31-05-2013	5690	2490	0.69	1544

Table 3.10: Measured concentration of PM_{10} at different receptors in the month of January and May 2013 for monthly averaging time period in µg/m^3

S. No.	Month	A1	A2	A3	A4
1.	January	4830	670	115	498
2.	May	2350	550	102	2490

Global coordinates of receptors were calculated in WGS, 1984 system using GPS. The location of high volume samplers is summarised Table 3.11.

Table 3.11: Location of Fine Dust Samplers

S. No.	Name of the location	X –Coordinate (m)	Y- Coordinate(m)
1.	*A1*	794255	2410945
2.	*A2*	793432	2411607
3.	*A3*	792856	2407284
4.	*A4*	792254	2410782

3.6 Validation of simulation model of a coal mine

PM_{10} concentration at different receptors near to the coal mine 'A' has been predicted by AERMOD. These results are further required to be validated from the measures concentration at the same receptors for same time averaging period. This has been done by using several statistical parameters those are discussed below.

3.6.1 Statistical parameters used for the validation study

Seven statistical parameters have been considered for the validation of simulation of a coal mine by AERMOD in a quantitative way. This model requires several independent and dependent parameters. The output from the model has been

measured in different time and space. Therefore following statistical parameters have been used for validation (Zou et al., 2010).

(i) Fractional Bias: The bias has been normalized to make it dimensionless. The fractional bias (FB) varies between -2 and +2 and has an ideal value of zero for an ideal model. Fractional Bias is a useful model performance indicator because it has the advantage of equally weighting positive and negative bias estimates (Singh et al., 2006). FB is given by

$$FB = 2\left(\frac{\overline{Co} - \overline{Cp}}{\overline{Co} + \overline{Cp}}\right) \qquad (6.1)$$

Where $Co\ is\ mean\ of\ observed\ concentrations\ of\ particulate\ matter.$

$Cp\ is\ mean\ of\ predicted\ concentrations\ of\ particulate\ matter.$

(ii) Fractional Variance: The fractional variance (FS) is a normalization of the mean bias of the variances of the observed and predicted values (Singh et al., 2006). The fractional variance is given by

$$FS = 2\left(\frac{\sigma_{Co} - \sigma_{Cp}}{\sigma_{Co} + \sigma_{Cp}}\right) \qquad (6.2)$$

Where,

$\sigma_{Co}\ is\ standard\ deviation\ of\ observed\ concentrations\ of\ particulate\ matter.$

$\sigma_{Cp}\ is\ standard\ deviation\ of\ \ predicted\ concentrations\ of\ particulate\ matter$

(iii) Normalised Mean Square Error: Normalized mean square error (NMSE) emphasizes the scatter in the entire set and is an estimator of the overall deviations between the observed and predicted values. Smaller values of NMSE indicate a better performance and it is not biased toward models that over predict or under predict (Mohan et al., 2011). The expression for NMSE is given by

$$NMSE = \frac{(\overline{Co} - \overline{Cp})^2}{Co \times Cp} \quad (6.3)$$

(iv) Coefficient of correlation: Correlation analysis involves statistical parameters obtained by linear least-squares regression. The value of correlation (*r*) close to 1 indicates perfect correlation between the observed and the predicted values that is a sign of good model performance (Mohan et al., 2011). The coefficient of correlation is given by

$$r = \frac{\overline{(Co - \overline{Co})(Cp - \overline{Cp})}}{\sigma_{Co}\sigma_{Cp}} \quad (6.4)$$

(v) Geometric Bias: There is large range of magnitude of observed and predicted concentrations, due to the use of field data with large distance distances from the source. This suggests the use of the geometric mean bias (MG) as an extra index for the determination of model overestimation or underestimation (Zou et al., 2010). The geometric mean parameter is estimated by the equation 6.5 as:

$$MG = exp\left(\overline{\ln Co} - \overline{\ln Cp}\right) \quad (6.5)$$

(vi) Geometric Variance: Similarly as the same reason for the calculation MG, Geometric Variance (VG) is also calculated for the large distance of the sources from the receptors (Zou et al., 2010). VG can be estimated as follows:

$$VG = exp\left(\overline{\ln Co - \ln Cp}\right)^2 \quad (6.6)$$

(vii) Index of agreement: The Index of Agreement (d) developed by Willmott (1981) as a standardized measure of the degree of model prediction error and varies between 0 and 1. A value of 1 indicates a perfect match, and 0 indicates no agreement at all (Willmott, 1981). The expression for index of agreement can be given as

$$d = 1 - \frac{\sum_{i=1}^{N}(\overline{Cp - Co})^2}{\sum_{i=1}^{N}(|Cp - \overline{Co}| + |Co - \overline{Co}|)^2} \quad (6.7)$$

Where, *N* is no. of measured or observed concentrations of particulate matter.

The difference between NMSE and'd' is that NMSE is a statistical performance measure that provides information about the actual value of error

produced by the model whereas 'd' measures the agreement between observed and predicted values (Sandu et al., 2005).

(viii) Quantile – Quantile (Q-Q) Plot: Q – Q plots are the cumulative frequency distributions that provides a graphical information of the distribution of observed and predicted values over their entire range (Danish, 2006). These plots determine whether the two sets of data come from same distribution or not. A model with a slope similar to that of 1:1 line and with values close to 1:1 line indicates that the predicted values are in good fit with the observed values (Zou et al., 2010). A solid line is usually used in the Q-Q plots to indicate an unbiased prediction and two dotted lines above and below to the 1:1line indicate the under and over prediction by the model respectively (Paine et al., 1998).

3.6.2 Model Performance Evaluation using Statistical Parameters

The set of statistical parameters, as discussed above, for different time averaging period has been calculated for all the four receptors. These parameters have been calculated for both the seasons. Table No. 3.12 summarises the values of statistical parameters calculated for model performance evaluation at daily averaging time period for the month of January 2013.

Table 3.12: Model performance statistics for simulated PM_{10} Concentrations at daily average at four receptors for January 2013

Receptors	Fractional Bias	Fractional Variance	Normalised Mean Square error	Coefficient of correlation	Geometric Bias	Geometric Variance	Index of Agreement
A1	0.797	-0.465	0.193	0.958	0.889	1.016	0.988
A2	1.381	-0.224	0.153	0.982	0.927	1.007	1
A3	1.294	0.066	0.643	0.93	0.851	1.033	1
A4	1.326	0.278	0.036	0.995	0.957	1.003	1

The statistical analysis of predicted concentrations for daily averaging period for all four receptors in the month of January 2013 has shown that fractional bias values were 0.797, 1.381, 1.294 and 1.326 for A1, A2, A3 and A4 receptor respectively as shown in Table no. 3.12. These values of FB are within the range of -2 to +2, which is desired for a good model. The best value of FB was found for A1 receptor in peak winter season.

The statistical analysis of predicted concentrations for daily averaging period for all four receptors in the month of January 2013 has shown that fractional variance values were -0.465, -0.224, 0.066 and 0.278 for A1, A2, A3 and A4 receptor respectively as shown in Table no. 3.12.The FS values are near to zero, which suggest the model performance is good and the least values of FS was found for the A3 receptor in peak winter season.

It is observed from Table No. 3.12 that NMSE values for daily averaging period for all four receptors in the month of January 2013 were 0.193, 0.153, 0.643 and 0.036 for A1, A2, A3 and A4 receptor respectively. Small values of NMSE suggests good performance of a model. The value of NMSE is observed to be least for A4 receptor in peak winter season.

The values of coefficient of correlation (r) has also been tabulated in Table no. 3.12 for daily averaging period for all four receptors in the month of January 2013. These were 0.958, 0.982, 0.93 and 0.995 for A1, A2, A3 and A4 receptor respectively. The values of 'r' closer to 1 suggests that model performance is very good for given time averaging period. The 'r' values were best for A4 receptor in peak winter season.

It could be observed from Table no 3.12 that Geometric Bias (MG) values for daily averaging period for all four receptors in the month of January 2013 were 0.889, 0.927, 0.851 and 0.957 for A1, A2, A3 and A4 receptors respectively. The values of MG near to 1 suggests that the model perform well for larger distance prediction. Almost all values are near to 1 whereas values of MG were best for A4 receptor in peak winter season.

It could also be observed from Table no 3.12 that Geometric Variance (VG) values for daily averaging period for all four receptors in the month of January 2013 1.016, 1.007, 1.033 and 1.003 for A1, A2, A3 and A4 receptor respectively. The values of VG near to 1 suggests that the model perform well for larger distance prediction.

Almost all values are near to 1 whereas values of VG were best for A4 receptor in peak winter season.

It can also be witnessed from Table no 3.12 that Index of agreement (d) values for daily averaging period for all four receptors in the month of January 2013 are 0.988, 1, 1 and 1 for A1, A2, A3 and A4 receptor respectively. The values of 'd' near to 1 suggests that the model perform well for given time and space. It also suggests that there is good agreement between measured and predicted values from a model. Almost all values are 1 or near to 1 of 'd' which suggests that the predicted concentrations are having good agreement at all receptors in peak winter season.

Table 3.13: Model performance statistics for simulated PM_{10} Concentrations at monthly average at four receptors for January 2013

Receptors	Fractional Bias	Normalised Mean Square error	Geometric Bias	Geometric Variance
A1	-0.106	0.011	0.955	1.002
A2	0.037	0.001	1.016	1
A3	0.218	0.048	1.01	1.009
A4	-0.151	0.023	0.937	1.004

The statistical analysis of predicted concentrations for monthly averaging period for all four receptors in the month of January 2013 has shown that fractional bias values were -0.106, 0.037, 0.218 and -0.151 for A1, A2, A3 and A4 receptor respectively as shown in Table no. 3.13. These values of FB are within the range of -2 to +2, which is desired for a good model. The best value of FB was found for the A2 receptor in peak winter season.

The statistical parameters Table No. 3.13 has shown that NMSE values for monthly averaging period for all four receptors in the month of January 2013 were 0.011, 0.001, 0.048 and 0.023 for A1, A2, A3 and A4 receptor respectively. Small

values of NMSE suggests good performance of a model. These values of NMSE were found least for A2 receptor in peak winter season.

It could be observed from Table no 3.13 that Geometric Bias (MG) values for monthly averaging period for all four receptors in the month of January 2013 were 0.955, 1.016, 1.01 and 0.937 for A1, A2, A3 and A4 receptor respectively. The values of MG near to 1 suggests that the model perform well for larger distance prediction. Almost all values are near to 1 whereas values of MG were best for A3 receptor in peak winter season.

It could also be observed from Table no 3.13 that Geometric Variance (VG) values monthly averaging period for all four receptors in the month of January 2013 1.002, 1, 1.009 and 1.004 for A1, A2, A3 and A4 receptor respectively. The values of VG near to 1 suggests that the model perform well for larger distance prediction. Almost all values are near to 1 whereas values of VG were best for A2 receptor in peak winter season.

Table 3.14: Model performance statistics for simulated PM_{10} Concentrations at daily average at four receptors for May 2013

Receptors	Fractional Bias	Fractional Variance	Normalised Mean Square error	Coefficient of correlation	Geometric Bias	Geometric Variance	Index of Agreement
A1	1.005	0.19	0.021	0.922	0.945	1.012	1
A2	1.208	-0.31	0.018	0.865	0.98	1.006	1
A3	1.325	0.143	0.489	0.995	0.883	1.016	1
A4	1.161	0.024	0.081	0.985	0.927	1.01	1

The statistical analysis of predicted concentrations for daily averaging period for all four receptors in the month of May 2013 has shown that fractional bias values were 1.005, 1.208, 1.325 and 1.161 for A1, A2, A3 and A4 receptor respectively as shown in Table no. 3.14. These values of FB are within the range of -2 to +2, which is

desired for a good model. The best value of FB was found for the A1 receptor in peak summer season.

The statistical analysis of predicted concentrations on daily basis in the month of May 2013 has shown that the fractional variance at all the four receptors A1, A2, A3 and A4 receptor was 0.19, -0.31, 0.143 and 0.024 respectively (Table no. 3.14). The least value of FS was obtained for the receptor A4 in peak summer season. The FS values are near to zero in general, which suggest that the model performance is good.

It is observed from Table No. 3.14 that NMSE values for daily averaging period for all four receptors in the month of May 2013 were 0.021, 0.018, 0.489 and 0.081 for A1, A2, A3 and A4 receptor respectively. Small values of NMSE suggests good performance of a model. The value of NMSE is observed to be least for A2 receptor in peak summer season.

The values of coefficient of correlation (r) has been tabulated in Table 3.14 for daily averaging period for all four receptors in the month of May 2013 were 0.922, 0.865, 0.995 and 0.985 for A1, A2, A3 and A4 receptor respectively. 'r' values closer to 1 suggests that model performance is very good for given time averaging period. The 'r' values were best for A3 receptor in peak summer season.

It could be observed from Table no 3.14 that Geometric Bias (MG) values for daily averaging period for all four receptors in the month of May 2013 were 0.945, 0.98, 0.883 and 0.927 for A1, A2, A3 and A4 receptor respectively. The values of MG near to 1 suggests that the model perform well for larger distance prediction. Almost all values are near to 1 whereas values of MG were best for A1 receptor in peak summer season.

It could also be observed from Table no 3.14 that Geometric Variance (VG) values for daily averaging period for all four receptors in the month of May 2013 1.012, 1.006, 1.016 and 1.01 for A1, A2, A3 and A4 receptor respectively. The values of VG near to 1 suggests that the model perform well for larger distance prediction. Almost all values are near to 1 whereas values of VG were best for A2 receptor in peak summer season.

It could also be witnessed from Table no 3.14 that Index of agreement (d) values for daily averaging period for all four receptors in the month of May 2013 were

1. The values of 'd' near to 1 suggests that the model perform well for given time and space. It also suggests that there is good agreement between measured and predicted values from a model. All values are 1 for this time averaging period which suggests that the predicted concentrations are having very good agreement at all receptors in peak summer season for this time averaging period.

Table 3.15: Model performance statistics for simulated PM_{10} Concentrations at monthly average at four receptors for May 2013

Receptors	Fractional Bias	Normalised Mean Square error	Geometric Bias	Geometric Variance
A1	-0.127	0.016	0.946	1.003
A2	-0.188	0.036	0.921	1.007
A3	0.091	0.008	1.04	1.002
A4	-0.069	0.005	0.97	1

The statistical analysis of predicted concentrations for monthly averaging period for all four receptors in the month of May 2013 has shown that fractional bias values were -0.127, -0.188, 0.091 and -0.069 for A1, A2, A3 and A4 receptor respectively as shown in Table no. 3.15. These values of FB are within the range of -2 to +2, which is desired for a good model. The best value of FB was found for the A4 receptor in peak summer season.

The statistical parameters Table No. 3.15 has shown that NMSE values for monthly averaging period for all four receptors in the month of May 2013 were 0.016, 0.036, 0.008 and 0.005 for A1, A2, A3 and A4 receptor respectively. Small values of NMSE suggests good performance of a model. These values of NMSE were found least for A4 receptor in peak summer season.

It could be observed from Table no 3.15 that Geometric Bias (MG) values for monthly averaging period for all four receptors in the month of May 2013 were 0.946, 0.921, 1.04 and 0.97 for A1, A2, A3 and A4 receptor respectively. The values of MG

near to 1 suggests that the model perform well for larger distance prediction. Almost all values are near to 1 whereas values of MG were best for A4 receptor in peak summer season.

It could also be perceived from Table no 3.15 that Geometric Variance (VG) values monthly averaging period for all four receptors in the month of May 1.003, 1.007, 1.002 and 1 for A1, A2, A3 and A4 receptor respectively. The values of VG near to 1 suggests that the model perform well for larger distance prediction. Almost all values are near to 1 whereas values of VG were best for A4 receptor in peak summer season.

The Q-Q plots for different time averaging period have been shown through figure 3.66 though 3.69.

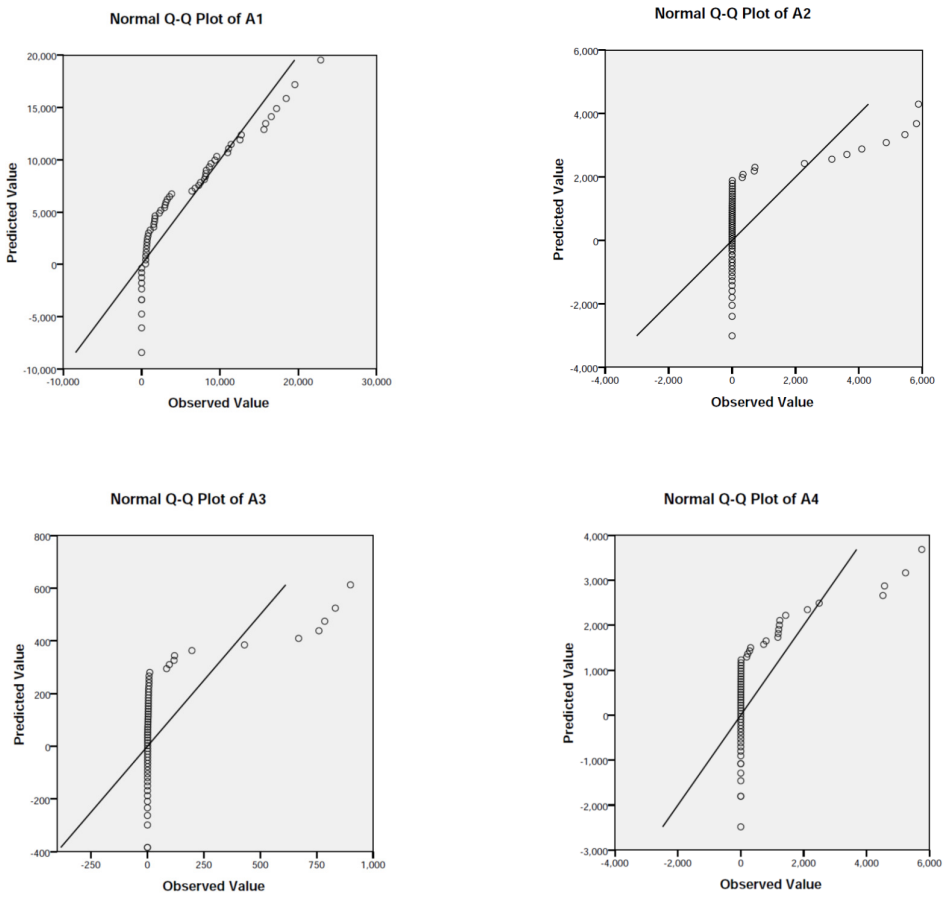

Figure 3.66: Q-Q plots of predicted and observed concentration for daily averaging time for all four receptors in the month of January 2013

It can be judged from Q-Q plots shown in figure 3.66 for daily averaging period that more values at A2 and A3 receptors are lying in a straight line along the Y- axis which are the lowest predicted values and repetitive in nature whereas for the A4 receptors these values are less in numbers. At A1 receptor, almost all the predicted and observed values are in good fit after leaving the lowest values and falls near to 1:1 line which further suggests that model performs best for A1 receptor in the given time and season.

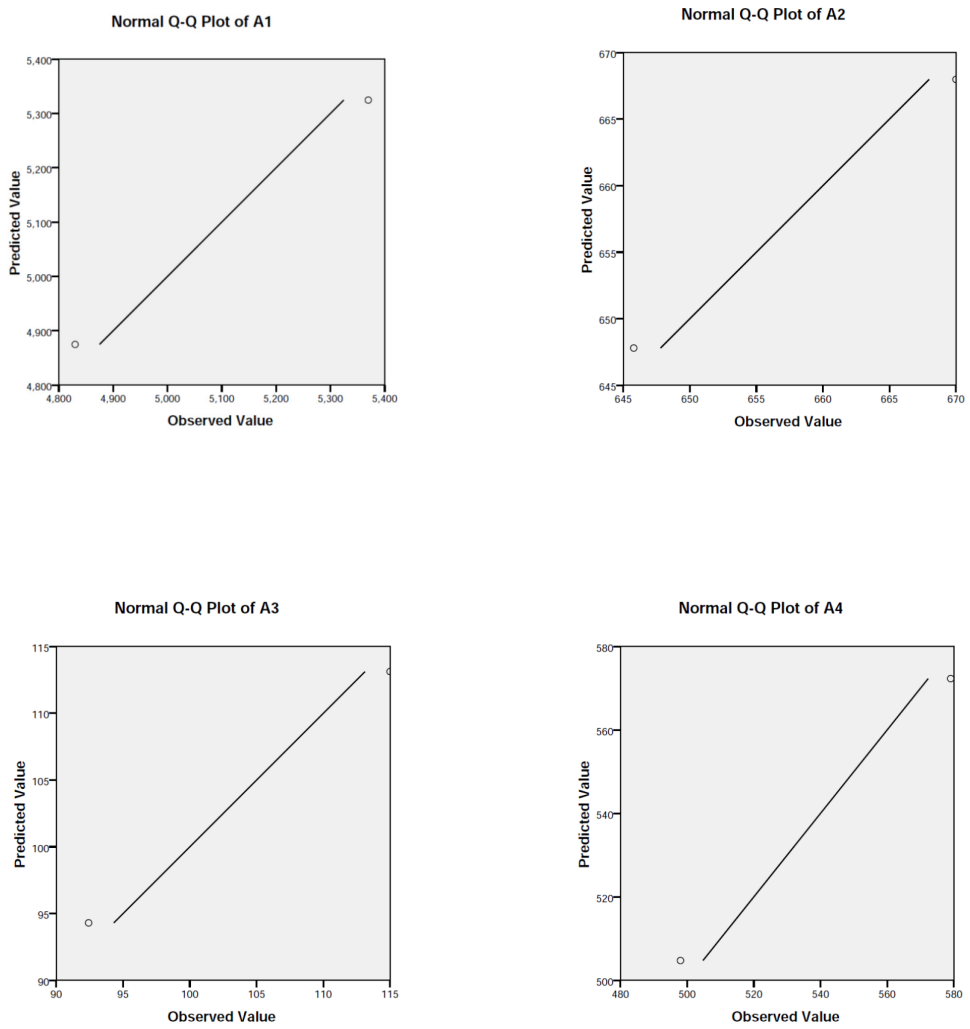

Figure 3.67: Q-Q plots of predicted and observed concentration for monthly averaging time for all four receptors in the month of January 2013

It can be judged from Q-Q plots shown in figure 3.67 for monthly averaging period that almost all the predicted and observed values for all four receptors are in good fit and falls near to 1:1 line which further suggests that model performs best for the given time and season.

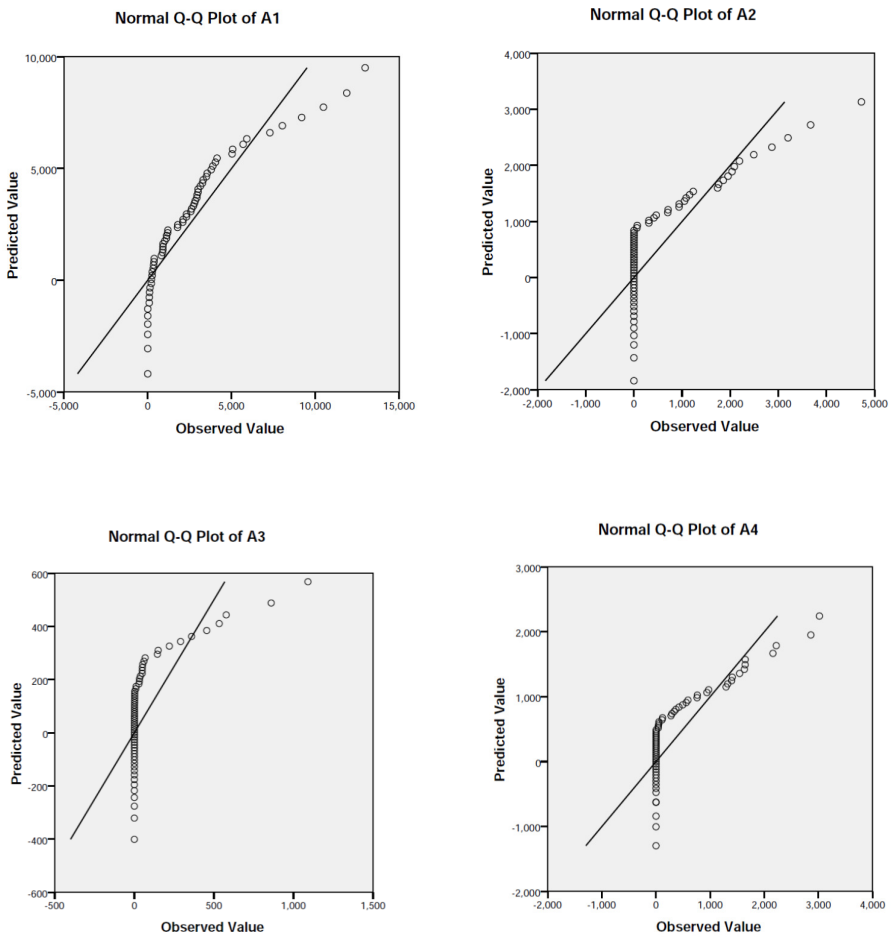

Figure 3.68: Q-Q plots of predicted and observed concentration for daily averaging time for all four receptors in the month of May 2013

It can be evaluated from Q-Q plots shown in figure 3.68 for daily averaging period that more values at A3 and A4 receptor are lying in a straight line along the Y-axis which are the lowest predicted values and repetitive in nature whereas for the A2 receptor these values are less in numbers. At A1 receptor, almost all the predicted and observed values are in good fit after leaving the lowest values and falls near to 1:1 line which further suggests that model performs best for A1 receptor in the given time and season.

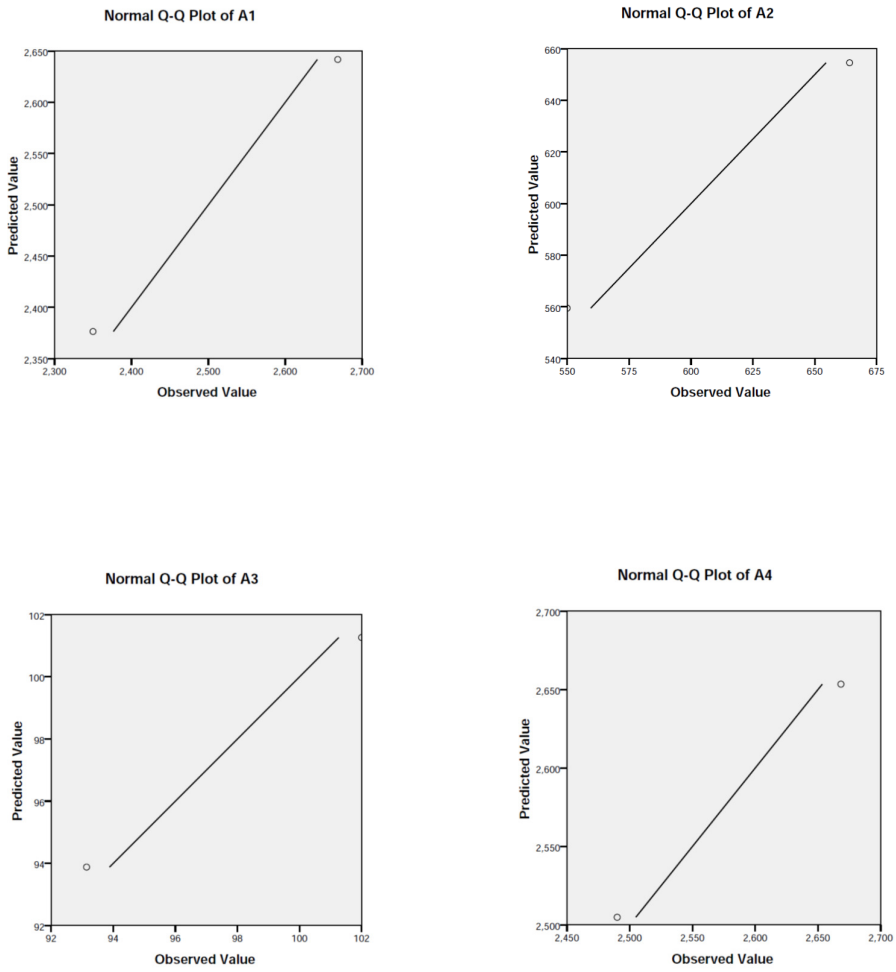

Figure 3.69: Q-Q plots of predicted and observed concentration for monthly averaging time for all four receptors in the month of May 2013

It can be judged from Q-Q plots shown in figure 3.69 for monthly averaging period that almost all the predicted and observed values for all four receptors are in good fit and falls near to 1:1 line which further suggests that model performs satisfactorily for the given time and season.